

Single-shot Hyper-parameter Optimization for Federated Learning: A General Algorithm & Analysis

Yi Zhou Parikshit Ram Theodoros Salonidis
Nathalie Baracaldo Horst Samulowitz Heiko Ludwig
IBM Research
{yi.zhou, Parikshit.Ram}@ibm.com
{tsaloni, baracald, samulowitz, hludwig}@us.ibm.com

February 18, 2022

Abstract

We address the relatively unexplored problem of hyper-parameter optimization (HPO) for federated learning (FL-HPO). We introduce **F**ederated **L**oss **S**urface **A**ggregation (**FLoRA**), a general FL-HPO solution framework that can address use cases of tabular data and any Machine Learning (ML) model including gradient boosting training algorithms and therefore further expands the scope of FL-HPO. **FLoRA** enables single-shot FL-HPO: identifying a single set of good hyper-parameters that are subsequently used in a *single* FL training. Thus, it enables FL-HPO solutions with minimal additional communication overhead compared to FL training without HPO. We theoretically characterize the optimality gap of **FLoRA**, which explicitly accounts for the heterogeneous non-iid nature of the parties' local data distributions, a dominant characteristic of FL systems. Our empirical evaluation of **FLoRA** for multiple ML algorithms on seven OpenML datasets demonstrates significant model accuracy improvements over the considered baseline, and robustness to increasing number of parties involved in FL-HPO training.

1 Introduction

Traditional machine learning (ML) approaches require training data to be gathered at a central location where the learning algorithm runs. In real world scenarios, however, training data is often subject to privacy or regulatory constraints restricting the way data can be shared, used and transmitted. Examples of such regulations include the European General Data Protection Regulation (GDPR), California Consumer Privacy Act (CCPA), Cybersecurity Law of China (CLA) and HIPAA, among others. Federated learning (FL), first proposed in McMahan et al. [2017b], has recently become a popular approach to address privacy concerns by allowing collaborative training of ML models among multiple parties where each party can keep its data private.

FL-HPO problem. Despite the privacy protection FL brings along, there are many open problems in FL domain [Kairouz et al., 2019, Khodak et al., 2021], one of which is hyper-parameter optimization for FL. Existing FL systems require a user (or all participating parties) to pre-set (agree on) multiple hyper-parameters (HPs) (i) for the model being trained (such as number of layers and batch size for neural networks or tree depth and number of trees in tree ensembles), and (ii) for the the aggregator (if such hyper-parameters exist). Hyper-parameter optimization (HPO) for FL is important because the choice of HPs can have dramatic impact on performance [McMahan et al., 2017b].

While HPO has been widely studied in the centralized ML setting, it comes with unique challenges in the FL setting. First, existing HPO techniques for centralized training often make use of the entire dataset, which is not available in FL. Secondly, they train a vast variety of models for a large number of HP configurations which would be prohibitively expensive in terms of communication and training time in FL settings. Thirdly, one important challenge that has not been adequately explored in FL literature is support for tabular data, which are widely used in enterprise settings [Ludwig et al., 2020]. One of the best models for this setting is based on gradient boosting tree algorithms [Friedman, 2001] which are different from the stochastic gradient descent algorithm used for neural networks. Recently, a few approaches have been proposed for FL-HPO, however they focus on handling HPO using personalization techniques [Khodak et al., 2021] and neural networks [Khodak et al., 2020]. To the best of our knowledge, there is no HPO approach for FL systems to train non-neural network models, such as XGBoost [Chen and Guestrin, 2016] that is particularly common in the enterprise setting.

Scope. In this paper, we address the aforementioned challenges of FL-HPO. We focus on the problem where the model HPs are shared across all parties and we seek a set of HPs and train a single model that is eventually used by all parties for testing/deployment. Moreover, we impose three further requirements that make the problem more challenging: **(C1)** we *do not make any assumption* that two models with different HPs can perform some form of “weight-sharing” (which is a common technique used in various HPO and neural architecture search (NAS) schemes for neural networks to reduce the computational overhead of HPO and NAS), allowing our solution to be applied beyond neural networks [Khodak et al., 2020]. **(C2)** we seek to **perform “single-shot”** FL-HPO, where we have *limited* resources (in the form of computation and communication overhead) which allow training only a single model via federated learning (that is, a single HP configuration), and **(C3)** we *do not assume that parties have independent and identically distributed (IID) data distributions*.

Contributions. Given the above FL-HPO problem setting, we make the following contributions:

- (§3) We present a novel framework **Federated Loss SuRface Aggregation (FLoRA)** that leverages meta-learning techniques to utilize **local and asynchronous** HPO on each party to perform single-shot HPO for the global FL-HPO problem.
- (§4) We provide theoretical guarantees for the set of HPs selected by FLoRA covering both IID and Non-IID cases. To the best of our knowledge, this is the first rigorous theoretical analysis for FL-HPO problem and also the first optimality gap constructed in terms of the estimated loss given a target distribution.
- (§5) We evaluate FLoRA on the FL-HPO of Gradient Boosted Decision Trees (GBDTs), Support Vector Machines (SVMs) and Multi-layered Perceptrons (MLPs) on seven classification datasets from OpenML [Vanschoren et al., 2013], highlighting (i) its performance relative to the baseline, (ii) the effect of various choices in this scheme, and (iii) the effect of the number of parties on the performance.

2 Related work

Performance optimization of FL systems. One of the main challenges in FL is achieving high accuracy and low communication overhead. FedAvg [McMahan et al., 2017a] is a predominant algorithm used for training in FL and several optimization schemes build on it. It is executed in multiple global rounds. At each round, the clients perform stochastic gradient descent (SGD) updates on their parameters based on their local objective functions. They subsequently send their updates to the server, which averages them and transmits their mean back to the clients. Several approaches have been devised for optimizing the communication performance of FL systems. Initially, communication optimizations included performing multiple SGD local iterations at the clients and randomly selecting a small subset of the clients to compute and send updates to the server [McMahan et al., 2017a]. Subsequently, compression techniques were used to minimize the size of model updates to the server. It

has been shown that the accuracy and communication performance of these techniques depend highly on their HPs [McMahan et al., 2017a].

FL-HPO approaches. Recent optimization approaches adapt HPs such as the local learning rate at each client [Koskela and Honkela, 2019, Mostafa, 2019, Reddi et al., 2020], the number of local SGD iterations (which affect the frequency of server updates) [Wang et al., 2019]. In Dai et al. [2020, 2021], Dai et.al. address Federated Bayesian Optimization. Although using HPO with multiple HPs, the problem setup is quite different than Federated Learning: they focus on a single party using information from other parties to accelerate its own Bayesian Optimization, instead of building a model for all parties. Federated Network Architecture Search (FNAS) approaches search for architectural HPs of deep learning CNN models by running locally NAS algorithms and then aggregating the NAS architecture weights and model weights using FedAvg [He et al., 2020, Garg et al., 2020, Xu et al., 2020]. These approaches have shown empirical gains but lack theoretical analysis. Inspired from the NAS technique of weight-sharing, [Khodak et al., 2020, 2021] proposed FedEx, a FL-HPO framework to accelerate a general HPO procedure, i.e., successive halving algorithm (SHA), for many SGD-based FL algorithms. Fedex focuses on building personalized models for parties by tuning local HPs of the parties. They provide a theoretical analysis for a special case of tuning a single HP (learning rate) in a convex optimization setting.

Our framework improves on the above approaches in several ways. **1) It is more general**, as it can tune multiple HPs and is applicable to non SGD-training settings such as gradient boosting trees. This is achieved by treating FL-HPO as a black-box HPO problem, which has been addressed in centralized HPO literature using grid search, random search [Bergstra and Bengio, 2012] and Bayesian Optimization approaches [Shahriari et al., 2016]. The key challenge is the requirement to perform computationally intensive evaluations on a large number of HPO configurations, where each evaluation involves training a model and scoring it on a validation dataset. In the distributed FL setting this problem is exacerbated because validation sets are local to the parties and each FL training/scoring evaluation is communication intensive. Therefore a brute force application of centralized black-box HPO approaches that select hyper-parameters in an outer loop and proceed with FL training evaluations is not feasible. **2) It yields minimal HPO communication overhead.** This is achieved by building a loss surface from local asynchronous HPO at the parties that yields a single optimized HP configuration used to train a global model with a single FL training. **3) It is the first that theoretically characterizes optimality gap in an FL-HPO setting**, for the case we focus in this paper (creating a global model by tuning multiple global HPs).

3 Methodology

In the centralized ML setting, we would consider a model class \mathcal{M} and its corresponding learning algorithm \mathcal{A} parameterized collectively with HPs $\theta \in \Theta$, and given a training set D , we can learn a single model $\mathcal{A}(\mathcal{M}, \theta, D) \rightarrow m \in \mathcal{M}$. Given some predictive loss $\mathcal{L}(m, D')$ of any model m scored on some holdout set D' , the centralized HPO problem can be stated as

$$\min_{\theta \in \Theta} \mathcal{L}(\mathcal{A}(\mathcal{M}, \theta, D), D'). \quad (3.1)$$

In the most general FL setting, we have p parties P_1, \dots, P_p each with their private local training dataset $D_i, i \in [p] = \{1, 2, \dots, p\}$. Let $D = \cup_{i=1}^p D_i$ denote the aggregated training dataset and $\bar{D} = \{D_i\}_{i \in [p]}$ denote the set of per-party datasets. Each model class (and corresponding learning algorithm) is parameterized by global HPs $\theta_G \in \Theta_G$ shared by all parties and per-party local HPs $\theta_L^{(i)} \in \Theta_L, i \in [p]$ with $\Theta = \Theta_G \times \Theta_L$. FL systems usually include an aggregator with its own set of HPs $\phi \in \Phi$. Finally, we would have a FL algorithm

$$\mathcal{F}(\mathcal{M}, \phi, \theta_G, \{\theta_L^{(i)}\}_{i \in [p]}, \mathcal{A}, \bar{D}) \rightarrow m \in \mathcal{M}, \quad (3.2)$$

which takes as input all the relevant HPs and per-party datasets and generates a model. In this case, the FL-HPO problem can be stated in the two following ways depending on the desired goals: (i) Ideally, for a global holdout dataset D' (a.k.a validation set, possibly from the same distribution as the aggregated dataset D), the target problem is:

$$\min_{\phi \in \Phi, \theta_G \in \Theta_G, \theta_L^{(i)} \in \Theta_L, i \in [p]} \mathcal{L} \left(\mathcal{F} \left(\mathcal{M}, \phi, \theta_G, \{\theta_L^{(i)}\}_{i \in [p]}, \mathcal{A}, \bar{D} \right), D' \right). \quad (3.3)$$

(ii) An alternative target problem would involve per-party holdout datasets $D'_i, i \in [p]$ as follows:

$$\min_{\phi \in \Phi, \theta_G \in \Theta_G, \theta_L^{(i)} \in \Theta_L, i \in [p]} \text{Agg} \left(\left\{ \mathcal{L} \left(\mathcal{F} \left(\mathcal{M}, \phi, \theta_G, \{\theta_L^{(i)}\}_{i \in [p]}, \mathcal{A}, \bar{D} \right), D'_i \right), i \in [p] \right\} \right), \quad (3.4)$$

where $\text{Agg} : \mathbb{R}^p \rightarrow \mathbb{R}$ is some aggregation function (such as average or maximum) that scalarizes the p per-party predictive losses.

Contrasting problem (3.1) to problems (3.3) & (3.4), we can see that the FL-HPO is significantly more complicated than the centralized HPO problem. In the ensuing presentation, we focus on problem (3.3) although our proposed single-shot FL-HPO scheme can be applied and evaluated for problem (3.4). We simplify the FL-HPO problem in the following ways: (i) we assume that there is no personalization so there are no per-party local HPs $\theta_L^{(i)}, i \in [p]$, (ii) we only focus on the model class HPs θ_G , deferring HPO for aggregator HPs ϕ for future work, and (iii) we assume there is a global holdout/validation set D' which is only used to evaluate the final global model's performance but *can not be accessed* during HPO process. Hence the problem we will study is stated as for a fixed aggregator HP ϕ :

$$\min_{\theta_G \in \Theta_G} \mathcal{L} \left(\mathcal{F} \left(\mathcal{M}, \phi, \theta_G, \mathcal{A}, \bar{D} \right), D' \right). \quad (3.5)$$

This problem appears similar to the centralized HPO problem (3.1). However, note that the main challenges in (3.5) is (i) the need for a federated training for each set of HPs θ_G , and (ii) the need to evaluate the trained model on the global validation set D' (which is usually not available in usual FL-HPO setting). Hence it is not practical (from a communication overhead and functional perspective) to apply existing off-the-shelf HPO schemes to problem (3.5). In the subsequent discussion, for simplicity purposes, we will use θ to denote the global HPs, dropping the ‘‘G’’ subscript.

3.1 Leveraging local HPOs

While it is impractical to apply off-the-shelf HPO solvers (such as Bayesian Optimization (BO) [Shahriari et al., 2016], Hyperopt [Bergstra et al., 2011], SMAC [Hutter et al., 2011], and such), we wish to understand how we can leverage local and asynchronous HPOs in each of the parties. We begin with a simple but intuitive hypothesis underlying various meta-learning schemes for HPO [Vanschoren, 2018, Wistuba et al., 2018]: *if a HP configuration θ has good performance for all parties independently, then θ is a strong candidate for federated training.*

With this hypothesis, we present our proposed algorithm FLoRA in Algorithm 1. In this scheme, we allow each party to perform HPO locally and asynchronously with some adaptive HPO scheme such as BO (line 3). Then, at each party $i \in [p]$, we collect all the attempted T HPs $\theta_t^{(i)}, t \in [T] = \{1, 2, \dots, T\}$ and their corresponding predictive loss $\mathcal{L}_t^{(i)}$ into a set $E^{(i)}$ (line 3, equation (3.6)). Then these per-party sets of (HP, loss) pairs $E^{(i)}$ are collected at the aggregator (line 5). This operation has at most $O(pT)$ communication overhead (note that the number of HPs are usually much smaller than the number of columns or number of rows in the per-party datasets). These sets are then used to generate an aggregated loss surface $\hat{\ell} : \Theta \rightarrow \mathbb{R}$ (line 6) which will then be used to make the final single-shot HP recommendation $\hat{\theta}^* \in \Theta$ (line 7) for the federated training to create the final model $m \in \mathcal{M}$ (line 8). We will discuss the generation of the aggregated loss surface in detail in §3.2. Before that, we briefly want to discuss the motivation behind some of our choices in Algorithm 1.

Algorithm 1 Single-shot FL-HPO with Federated Loss Surface Aggregation (FLoRA)

- 1: **Input:** $\Theta, \mathcal{M}, \mathcal{A}, \mathcal{F}, \{(D_i, D'_i)\}_{i \in [p]}, T$
- 2: **for** each party $P_i, i \in [p]$ **do**
- 3: Run HPO to generate T (HP, loss) pairs

$$E^{(i)} = \left\{ (\theta_t^{(i)}, \mathcal{L}_t^{(i)}), t \in [T] \right\}, \quad (3.6)$$

where $\theta_t^{(i)} \in \Theta, \mathcal{L}_t^{(i)} := \mathcal{L}(\mathcal{A}(\mathcal{M}, \theta_t^{(i)}, D_i), D'_i)$.

- 4: **end for**
- 5: Collect all $E = \{E^{(i)}, i \in [p]\}$ in aggregator
- 6: Generate a unified loss surface $\hat{\ell} : \Theta \rightarrow \mathbb{R}$ using E
- 7: Select best HP candidate

$$\hat{\theta}^* \leftarrow \arg \min_{\theta \in \Theta} \hat{\ell}(\theta). \quad (3.7)$$

- 8: Invoke federated training $m \leftarrow \mathcal{F}(\mathcal{M}, \hat{\theta}^*, \mathcal{A}, \bar{D})$
 - 9: **Output:** FL model m .
-

Why adaptive HPO? The reason to use adaptive HPO schemes instead of non-adaptive schemes such as random search or grid search is that this allows us to efficiently approximate the local loss surface more accurately (and with more certainty) in regions of the HP space where the local performance is favorable instead of trying to approximate the loss surface well over the complete HP space. This has advantages both in terms of computational efficiency and loss surface approximation.

Why asynchronous HPO? Each party executes HPO asynchronously, without coordination with HPO results from other parties or with the aggregator. This is in line with our objective to minimize communication overhead. Although there could be strategies that involve coordination between parties, they could involve many rounds of communication. Our experimental results show that this approach is effective for the datasets we evaluated for.

3.2 Loss surface aggregation

Given the sets of (HP, loss) pairs $E^{(i)} = (\theta_t^{(i)}, \mathcal{L}_t^{(i)}), i \in [p], t \in [T]$ at the aggregator, we wish to construct a loss surface $\hat{\ell} : \Theta \rightarrow \mathbb{R}$ that best emulates the (relative) performance loss $\hat{\ell}(\theta)$ we would observe when training the model on \bar{D} . Based on our hypothesis, we want the loss surface to be such that it would have a relatively low $\hat{\ell}(\theta)$ if θ has a low loss for all parties simultaneously. However, because of the asynchronous and adaptive nature of the local HPOs, for any HP $\theta \in \Theta$, we would not have the corresponding losses from all the parties. For that reason, we will model the loss surfaces using regressors that try to map any HP to their corresponding loss. In the following, we present four ways of constructing such loss surfaces:

Single global model (SGM). We merge all the sets $E = \cup_{i \in [p]} E^{(i)}$ and use it as a training set for a regressor $f : \Theta \rightarrow \mathbb{R}$, which considers the HPs $\theta \in \Theta$ as the covariates and the corresponding loss as the dependent variable. For example, we can train a random forest regressor [Breiman, 2001] on this training set E . Then we can define the loss surface $\hat{\ell}(\theta) := f(\theta)$. While this loss surface is simple to obtain, it may not be able to handle Non-iid party data distribution well: it is actually overly optimistic – under the assumption that every party generates unique HPs during the local HPO, this single global loss surface would assign a low loss to any HP θ which has a low loss at any one of the parties. This

implies that this loss surface would end up recommending HPs that have low loss in just one of the parties, but not necessarily on all parties.

Single global model with uncertainty (SGM+U). Given the merged set $E = \cup_{i \in [p]} E^{(i)}$, we can train a regressor that provides uncertainty quantification around its predictions (such as Gaussian Process Regressor [Williams and Rasmussen, 2006]) as $f : \Theta \rightarrow \mathbb{R}, u : \Theta \rightarrow \mathbb{R}_+$, where $f(\theta)$ is the mean prediction of the model at $\theta \in \Theta$ while $u(\theta)$ quantifies the uncertainty around this prediction $f(\theta)$. We define the loss surface as $\hat{\ell}(\theta) := f(\theta) + \alpha \cdot u(\theta)$ for some $\alpha > 0$. This loss surface does prefer HPs that have a low loss even in just one of the parties, but it penalizes a HP if the model estimates high uncertainty around this HP. Usually, a high uncertainty around a HP would be either because the training set E does not have many samples around this HP (implying that many parties did not view the region containing this HP as one with low loss), or because there are multiple samples in the region around this HP but parties do not collectively agree that this is a promising region for HPs. Hence this makes SGM+U more desirable than SGM, giving us a loss surface that estimates low loss for HPs that are simultaneously thought to be promising to multiple parties.

Maximum of per-party local models (MPLM). Instead of a single global model on the merged set E , we can instead train a regressor $f^{(i)} : \Theta \rightarrow \mathbb{R}, i \in [p]$ with each of the per-party set $E^{(i)}$. Given this, we can construct the loss surface as $\hat{\ell}(\theta) := \max_{i \in [p]} f^{(i)}(\theta)$. This can be seen as a much more pessimistic loss surface, assigning a low loss to a HP only if it has a low loss estimate across all parties.

Average of per-party local models (APLM). A less pessimistic version of MPLM would be to construct the loss surface as the average of the per-party regressors $f^{(i)}, i \in [p]$ instead of the maximum, defined as $\hat{\ell}(\theta) := 1/p \sum_{i=1}^p f^{(i)}(\theta)$. This is also less optimistic than SGM since it will assign a low loss for a HP only if its average across all per-party regressors is low, which implies that all parties observed a relatively low loss around this HP.

Intuitively, we believe that loss surfaces such as SGM+U or APLM would be the most promising while the extremely optimistic and pessimistic SGM and MPLM respectively would be relatively less promising, with MPLM being superior to SGM. In the following section, we theoretically quantify the performance guarantees for MPLM and APLM, and in §5, we evaluate all these loss surface empirically in the single-shot FL-HPO setting.

4 Optimality analysis

In this section, we provide a rigorous analysis of the sub-optimality of the HP selected by FLoRA. Let us first define some notation we will use throughout this section.

Definition 4.1 (Loss functions). For a given set of parties' data $\bar{D} = \{D_i\}_{i \in [p]}$ and any $\theta \in \Theta$, the true target loss (any predictive performance metric, such as, the training loss) can be expressed as:

$$\ell(\theta, \mathcal{D}) := \underbrace{\mathbb{E}_{(x,y) \sim \mathcal{D}}}_{\text{test perf. of trained model}} \mathcal{L}(\underbrace{\mathcal{A}(\theta, \bar{D})}_{\text{trained model}}, (x, y)). \tag{4.1}$$

Here \mathcal{D} is the data distribution of the test points. Let $\tilde{\ell}(\theta, \mathcal{D})$ be an estimate of the loss defined in (4.1) given some validation (holdout) set \mathcal{D}' sampled from \mathcal{D} , which is the model performance metric during evaluation and/or inference time.

We assume the parties' training sets are collected before the federated learning such that \bar{D} is fixed and unchanged during the HPO and FL processes, in order words, we do not consider streaming data setting.

Now we are ready to provide a more general definition of the unified loss surface constructed by FLoRA as follows:

Definition 4.2 (Unified loss surface). Given the local loss surfaces $\widehat{\ell}_i : \Theta \rightarrow \mathbb{R}$ for each party $i \in [p]$ generated by T (HP, loss) pairs $\{(\theta_t^{(i)}, \mathcal{L}_t^{(i)})\}_{t \in [T]}$, we can define the global loss surface $\widehat{\ell} : \Theta \rightarrow \mathbb{R}$ as

$$\widehat{\ell}(\theta) = \sum_{i=1}^p \alpha_i(\theta) \cdot \widehat{\ell}_i(\theta), \alpha_i(\theta) \in [0, 1], \sum_{i=1}^p \alpha_i(\theta) = 1. \quad (4.2)$$

In particular,

- i) If $\alpha_i(\theta) = 1/p, \forall i \in [p], \theta \in \Theta$, then this reduces to APLM loss surface.
- ii) If $\alpha_i(\theta) = \mathbb{I}(\widehat{\ell}_i(\theta) = \max_{j \in [p]} \widehat{\ell}_j(\theta))$, then this reduces to the MPLM loss surface (assuming all $\widehat{\ell}_j(\theta)$ s are unique).

We formalize the distance metric used in our analysis to evaluate the distance between two given data distributions.

Definition 4.3 (1-Wasserstein distance [Villani, 2003]). For two distributions μ, ν with bounded support, the 1-Wasserstein distance is defined as

$$\mathcal{W}_1(\mu, \nu) := \sup_{f \in F_1} \mathbb{E}_{x \sim \mu} f(x) - \mathbb{E}_{x \sim \nu} f(x), \quad (4.3)$$

where $F_1 = \{f : f \text{ is continuous, Lipschitz}(f) \leq 1\}$.

To facilitate our analysis later, we make the following Lipschitzness assumptions regarding the loss function $\widehat{\ell}$ and also the per-party loss surface $\widehat{\ell}_i$.

Assumption 4.4 (Lipschitzness). For a fixed data distribution \mathcal{D} and $\forall \theta, \theta' \in \bar{\Theta} \subset \Theta$, we have

$$|\tilde{\ell}(\theta, \mathcal{D}) - \tilde{\ell}(\theta', \mathcal{D})| \leq \tilde{L}(\mathcal{D}) \cdot d(\theta, \theta'), \quad (4.4)$$

$$|\widehat{\ell}_i(\theta) - \widehat{\ell}_i(\theta')| \leq \widehat{L}_i \cdot d(\theta, \theta'), \quad (4.5)$$

where $d(\cdot, \cdot)$ is a certain distance metric defined over the hyper-parameter search space, see Appendix A.1 for one definition. For a fixed set of hyper-parameters $\theta \in \bar{\Theta} \subset \Theta$ and some data distributions \mathcal{D} and \mathcal{D}' , we have

$$|\tilde{\ell}(\theta, \mathcal{D}) - \tilde{\ell}(\theta, \mathcal{D}')| \leq \tilde{\beta}(\theta) \cdot \mathcal{W}_1(\mathcal{D}, \mathcal{D}'). \quad (4.6)$$

Remark. Note that we explicitly use a $\bar{\Theta} \subset \Theta$ to highlight that we need Lipschitz-ness only in particular parts of the HP space. In fact, our analysis only requires the Lipschitz-ness at $\widehat{\theta}^*$, the optimal HP and a HP space containing these two HPs and the set of HP tried in local HPO runs, i.e., $\theta_t^{(i)}$, which most of the time does not cover the entire HP search space. Moreover, the above Lipschitzness assumption w.r.t. a general HP space, which could be a combination of continuous and discrete variables, may be strong. We also show in Appendix A.2 and B.4 that it can be relaxed to a milder assumption based on the modulus of continuity without significantly affecting our main results. For simplicity, we can always assume that $\tilde{L}(\mathcal{D}) \leq \tilde{L}, \forall \mathcal{D}$ and $\tilde{\beta}(\theta) \leq \tilde{\beta}, \forall \theta$.

Recall that the HP $\widehat{\theta}^*$ selected by FLoRA is defined as in (3.7). We then define the optimal HP given by the estimated loss function for a desired data distribution \mathcal{D} we want to learn as,

$$\theta^* \in \arg \min_{\theta \in \Theta} \tilde{\ell}(\theta, \mathcal{D}). \quad (4.7)$$

We are interested in providing a bound for the following *optimality gap*:

$$\tilde{\ell}(\widehat{\theta}^*, \mathcal{D}) - \tilde{\ell}(\theta^*, \mathcal{D}). \quad (4.8)$$

Note that this bound is the optimality gap for the output of FLoRA in terms of the estimated loss $\tilde{\ell}$. We state our main results in the following theorem. Informally speaking we show how to bound the optimality gap by picking the ‘worst-case’ HP setting that maximizes the combination of Wasserstein distances of the local data distributions and actual quality of local HPO approximation across parties.

Theorem 4.5. Consider the optimality gap defined in (4.8), where $\widehat{\boldsymbol{\theta}}^*$ is selected by FLoRA with each party $i \in [p]$ collecting \mathbb{T} (HP, loss) pairs $\{(\boldsymbol{\theta}_t^{(i)}, \mathcal{L}_t^{(i)})\}_{t \in [\mathbb{T}]}$ during the local HPO run. For a desired data distribution $\mathcal{D} = \sum_{i=1}^p w_i \mathcal{D}_i$, where $\{\mathcal{D}_i\}_{i \in [p]}$ are the sets of parties' local data distributions and $w_i \in [0, 1], \forall i \in [p]$, we have

$$\begin{aligned} & \tilde{\ell}(\widehat{\boldsymbol{\theta}}^*, \mathcal{D}) - \tilde{\ell}(\boldsymbol{\theta}^*, \mathcal{D}) \\ & \leq 2 \max_{\boldsymbol{\theta} \in \Theta} \sum_{i \in [p]} \alpha_i(\boldsymbol{\theta}) \left\{ \tilde{\beta}(\boldsymbol{\theta}) \sum_{j \in [p], j \neq i} w_j \mathcal{W}_1(\mathcal{D}_j, \mathcal{D}_i) + \left(\tilde{\mathcal{L}}(\mathcal{D}_i) + \widehat{\mathcal{L}}_i \right) \min_{t \in [\mathbb{T}]} d(\boldsymbol{\theta}, \boldsymbol{\theta}_t^{(i)}) + \delta_i \right\}, \end{aligned} \quad (4.9)$$

where δ_i is the maximum per sample training error for the local loss surface $\widehat{\ell}_i$, i.e., $\delta_i = \max_t |\mathcal{L}_t^{(i)} - \widehat{\ell}_i(\boldsymbol{\theta}_t^{(i)})|$. In particular, when all parties have i.i.d. local data distributions, (4.9) reduces to

$$\tilde{\ell}(\widehat{\boldsymbol{\theta}}^*, \mathcal{D}) - \tilde{\ell}(\boldsymbol{\theta}^*, \mathcal{D}) \leq 2 \max_{\boldsymbol{\theta} \in \Theta} \sum_{i=1}^p \alpha_i(\boldsymbol{\theta}) \left\{ \left(\tilde{\mathcal{L}}(\mathcal{D}_i) + \widehat{\mathcal{L}}_i \right) \min_{t \in [\mathbb{T}]} d(\boldsymbol{\theta}, \boldsymbol{\theta}_t^{(i)}) + \delta_i \right\}.$$

We make some observations regarding the above results. Firstly, the first term in our bound characterizes the errors incurred by the differences among parties' local data distributions, i.e., the magnitude of Non-IIDness in a FL system. In particular, we can see it vanish under the IID setting. Secondly, the last two terms measure the quality of the local HPO approximation, which can be reduced if a good loss surface is selected. Thirdly, $\min_{t \in [\mathbb{T}]} d(\boldsymbol{\theta}, \boldsymbol{\theta}_t^{(i)})$ indicates that the optimality gap depends only on the HP trials $\boldsymbol{\theta}_t^{(i)}$ that is closest to the optimal HP setting. Finally, if we assume each party's training dataset \mathcal{D}_i is of size n_i sampled as $\mathcal{D}_i \sim \mathcal{D}_i^{n_i}$, we can view $w_i = \frac{n_i}{n}$ where $n = \sum_{i=1}^p n_i$, i.e., with probability w_i the desired data distribution \mathcal{D} is sampled from \mathcal{D}_i .

In order to obtain the result in (4.9), we first analyze (4.8) in Proposition 4.6, see its proof in Appendix B. Note that the local loss surfaces $\widehat{\ell}_i$, $i \in [p]$ are computed at a certain test/validation set sampled from the parties local data distribution \mathcal{D}_i . We quantify the relationship between $\widehat{\ell}_i(\boldsymbol{\theta})$ and the estimated loss function $\tilde{\ell}(\boldsymbol{\theta}, \mathcal{D}_i)$ as follows:

$$|\widehat{\ell}_i(\boldsymbol{\theta}) - \tilde{\ell}(\boldsymbol{\theta}, \mathcal{D}_i)| := \epsilon_i(\boldsymbol{\theta}, \mathbb{T}). \quad (4.10)$$

Proposition 4.6. Consider $\widehat{\boldsymbol{\theta}}^*$ and $\boldsymbol{\theta}^*$ are two sets of HP defined in (3.7) and (4.7), respectively, and $\{\mathcal{D}_i\}_{i \in [p]}$ and \mathcal{D} are the sets of parties' local data distributions and the target (global) data distribution we want to learn, for a given HP space such that $\widehat{\boldsymbol{\theta}}^*, \boldsymbol{\theta}^* \in \Theta \subset \Theta$, we have

$$\tilde{\ell}(\widehat{\boldsymbol{\theta}}^*, \mathcal{D}) - \tilde{\ell}(\boldsymbol{\theta}^*, \mathcal{D}) \leq 2 \max_{\boldsymbol{\theta} \in \Theta} \sum_{i \in [p]} \alpha_i(\boldsymbol{\theta}) \left\{ \tilde{\beta}(\boldsymbol{\theta}) \mathcal{W}_1(\mathcal{D}, \mathcal{D}_i) + \epsilon_i(\boldsymbol{\theta}, \mathbb{T}) \right\}. \quad (4.11)$$

We now dive into each term in (4.11) to provide tight bounds for $\mathcal{W}_1(\mathcal{D}, \mathcal{D}_i)$ and $\epsilon_i(\boldsymbol{\theta}, \mathbb{T})$ in the following propositions. All the proofs can be found in Appendix B.

Proposition 4.7. Consider 1-Wasserstein distance we defined in (4.3), for a local data distribution \mathcal{D}_i of any party i , $i \in [p]$, and $\mathcal{D} = \sum_{i=1}^p w_i \mathcal{D}_i$ for some $w_i \in [0, 1], \forall i \in [p]$, we have

$$\mathcal{W}_1(\mathcal{D}, \mathcal{D}_i) \leq \sum_{j \in [p], j \neq i} w_j \mathcal{W}_1(\mathcal{D}_j, \mathcal{D}_i). \quad (4.12)$$

In particular, when \mathcal{D}_i , $i \in [p]$ are i.i.d. data distribution, i.e., all parties in a federated learning system possess i.i.d. local data distribution - that is, $\mathcal{W}_1(\mathcal{D}_j, \mathcal{D}_i) = 0 \forall i, j \in [p]$ - then $\sum_{j \in [p], j \neq i} w_j \mathcal{W}_1(\mathcal{D}_j, \mathcal{D}_i) = 0$. Therefore, $\mathcal{W}_1(\mathcal{D}, \mathcal{D}_i) = 0, \forall i \in [p]$.

Proposition 4.8. For any party i , $i \in [p]$, consider a (HP, loss) pair $(\boldsymbol{\theta}_t^{(i)}, \mathcal{L}_t^{(i)})$ collected during the local HPO run for party i , for any $\boldsymbol{\theta} \in \Theta \subset \Theta$, we have

$$\epsilon_i(\boldsymbol{\theta}, \mathbb{T}) \leq \left(\tilde{\mathcal{L}}(\mathcal{D}_i) + \widehat{\mathcal{L}}_i \right) \min_{t \in [\mathbb{T}]} d(\boldsymbol{\theta}, \boldsymbol{\theta}_t^{(i)}) + \delta_i, \quad (4.13)$$

where $\delta_i = \max_t |\mathcal{L}_t^{(i)} - \widehat{\ell}_i(\boldsymbol{\theta}_t^{(i)})|$ is the maximum per sample training error for the local loss surface $\widehat{\ell}_i$.

Table 1: Comparison of different loss surfaces (the 4 rightmost columns) for FLoRA relative to the baseline for single-shot 3-party FL-HPO in terms of the *relative regret* (lower is better).

| Aggregate | ML Method | SGM | SGM+U | MPLM | APLM |
|---------------------------|-----------|---------------------------|--------------------|--------------------|---------------------------|
| Regret | HGB | [0.30, 0.47, 0.68] | [0.27, 0.54, 0.64] | [0.25, 0.43, 0.67] | [0.25, 0.50, 0.65] |
| Inter-quartile range | SVM | [0.04, 0.38, 1.11] | [0.04, 0.48, 1.07] | [0.38, 0.91, 2.41] | [0.23, 0.54, 0.76] |
| | MLP | [0.36, 0.80, 0.97] | [0.48, 0.99, 1.01] | [0.47, 0.89, 1.00] | [0.46, 0.79, 0.95] |
| | Overall | [0.22, 0.53, 0.97] | [0.32, 0.55, 1.01] | [0.36, 0.61, 0.99] | [0.36, 0.57, 0.79] |
| FLoRA | HGB | 6/0/1 | 6/0/1 | 7/0/0 | 7/0/0 |
| Wins/Ties/Losses | SVM | 4/0/2 | 4/0/2 | 3/0/3 | 5/0/1 |
| | MLP | 6/0/1 | 4/1/2 | 5/1/1 | 6/0/1 |
| | Overall | 16/0/4 | 14/1/5 | 15/1/4 | 18/0/2 |
| Wilcoxon Signed-Rank Test | HGB | (26, 0.02126) | (27, 0.01400) | (28, 0.00898) | (28, 0.00898) |
| 1-sided | SVM | (18, 0.05793) | (17, 0.08648) | (9, 0.62342) | (15, 0.17272) |
| (statistic, p-value) | MLP | (21, 0.11836) | (15, 0.17272) | (18, 0.05793) | (24, 0.04548) |
| | Overall | (174, 0.00499) | (164, 0.00272) | (141, 0.03206) | (183.5, 0.00169) |

Note that if we use non-parametric regression models as the loss surfaces (such as Gaussian Processes, Random Forests, etc), the per-sample training error can be made arbitrarily small (that is $\delta_i \approx 0$), but at the cost of increasing \widehat{L}_i for $\widehat{\ell}_i$.

5 Empirical evaluation

In this section, we evaluate our proposed scheme FLoRA with different loss surfaces for the FL-HPO on a variety of ML models – histograms based gradient boosted (HGB) decision trees [Friedman, 2001], Support Vector Machines (SVM) with RBF kernel and multi-layered perceptrons (MLP) (using their respective `scikit-learn` implementation [Pedregosa et al., 2011]) on OpenML [Vanschoren et al., 2013] classification problems. The precise HP search space is described in Appendix C.2. First, we fix the number of parties $p = 3$ and compare FLoRA to a baseline on 7 datasets. Then we study the effect of increasing the number of parties from $p = 3$ up to $p = 100$ on the performance of our proposed scheme on 3 datasets. The data is randomly split across parties. We also evaluate FLoRA with different parameter choices, in particular, the number of local HPO rounds and the communication overhead in the aggregation of the per-party (HP, loss) pairs. Finally, we evaluate FLoRA in a real FL testbed IBM FL [Ludwig et al., 2020] using its default HP setting as a baseline. More experimental results can be found in Appendix C.

Single-shot baseline. To appropriately evaluate our proposed single-shot FL-HPO scheme, we need to select a meaningful single-shot baseline. For this, we choose the default HP configuration of `scikit-learn` as the single-shot baseline for two main reasons: (i) the default HP configuration in `scikit-learn` is set manually based on expert prior knowledge and extensive empirical evaluation, and (ii) these are also used as the defaults in the Auto-Sklearn package [Feurer et al., 2015, 2020], one of the leading open-source AutoML python packages, which maintains a carefully selected portfolio of default configurations.

Dataset selection. For our evaluation of single-shot HPO, we consider 7 binary classification datasets of varying sizes and characteristics from OpenML [Vanschoren et al., 2013] such that there is at least a significant room for improvement over the single-shot baseline performance. We consider datasets which have at least $> 3\%$ potential improvement in balanced accuracy for gradient boosted decision trees. See Appendix C.1 for details on data. Note that this only ensures room for improvement for HGB, while highlighting cases with no room for improvement for SVM and MLP as we see in our results.

(Dis-)Regarding other baselines. While there are some existing schemes for FL-HPO (as discussed in §2), we are unable to compare FLoRA to them for the following reasons: (i) As noted by Khodak et al.

[2021, Section 1, Related Work], existing schemes focus “on a small number of hyperparameters (e.g. the step-size and sometimes one or two more) in less general settings (studying small-scale problems or assuming server-side validation data)” whereas we explicitly assume no access to such a “server-side validation data”. (ii) Furthermore, we noted in §1 (**C1**), we do not assume any “weight-sharing” type capability, and hence it is not clear how FedEx [Khodak et al., 2021] can be applied to FL-HPO in the general¹.

Implementation. We consider two implementations for our empirical evaluation. In our first three sets of experiments, we emulate the final FL (Algorithm 1, line 8) with a centralized training using the pooled data. We chose this implementation because we want to evaluate the final performance of any HP configuration (baseline or recommended by FLoRA) in a statistically robust manner with multiple train/validation splits (for example, via 10-fold cross-validation) instead of evaluating the performance on a single train/validation. This form of evaluation is extremely expensive to perform in a real FL system and generally not feasible, but allows us to evaluate how the performance of our single-shot HP recommendation fairs against that of the best-possible HP found via a full-scale centralized HPO.

Evaluation metric. In all datasets, we consider the balanced accuracy as the metric we wish to maximize. For the local per-party HPOs (as well as the centralized HPO we execute to compute the regret), we maximize the 10-fold cross-validated balanced accuracy. For Table 1-2, we report the *relative regret*, computed as $(\mathbf{a}^* - \mathbf{a}) / (\mathbf{a}^* - \mathbf{b})$, where \mathbf{a}^* is the best metric obtained via the centralized HPO, \mathbf{b} is the result of the baseline, and \mathbf{a} is the result of the HP recommended by FLoRA. The baseline has a relative regret of 1 and smaller values imply better performance. A value larger than 1 implies that the recommended HP performs worse than the baseline.

Comparison to single-shot baseline. In our first set of experiments for 3-party FL-HPO ($p = 3$), we compare our proposed scheme with the baseline across different datasets, machine learning models and FLoRA loss surfaces. The aggregated results are presented in Table 1, with the individual results detailed in Appendix C.3. For each of the three methods, we report the aggregate performance over all considered datasets in terms of (i) inter-quartile range, (ii) Wins/Ties/Losses of FLoRA w.r.t. the single-shot baseline, and (iii) a one-sided Wilcoxon Signed Ranked Test of statistical significance with the null hypothesis that the median of the difference between the single-shot baseline and FLoRA is positive against the alternative that the difference is negative (implying FLoRA improves over the baseline). Finally, we also report an “Overall” performance, further aggregated across all ML models.

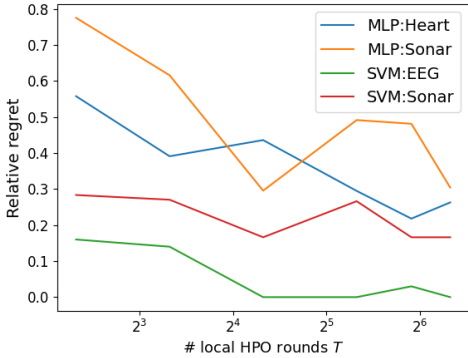
All FLoRA loss surfaces show strong performance w.r.t the single-shot baseline, with significantly more wins than losses, and 3rd-quartile relative regret values less than 1 (indicating improvement over the baseline). All FLoRA loss surfaces have a p-value of less than 0.05, indicating that we can reject the null hypothesis. Overall, APLM shows the best performance over all loss surfaces, both in terms of Wins/Ties/Losses over the baseline as well as in terms of the Wilcoxon Signed Rank Test, with the highest statistic and a p-value close to 10^{-3} . APLM also has significantly lower 3rd-quartile than all other loss surfaces. MPLM appears to have the worst performance but much of that is attributable to a couple of very hard cases with SVM (see Appendix C.3 for detailed discussion). Otherwise, MPLM performs second best both for FL-HPO with HGB and MLP.

Effect of increasing number of parties. In the second set of experiments, we study the effect of increasing the number of parties in the FL-HPO problem on 3 datasets and HGB. For each data set, we increase the number of parties p up until each party has at least 100 training samples. We present the relative regrets in Table 2. It also displays $\gamma_p := (1 - \min_{i \in [p]} \mathcal{L}_*^{(i)}) / (1 - \max_{i \in [p]} \mathcal{L}_*^{(i)})$, where $\mathcal{L}_*^{(i)} = \min_{t \in [T]} \mathcal{L}_t^{(i)}$ is the minimum loss observed during the local asynchronous HPO at party i . This

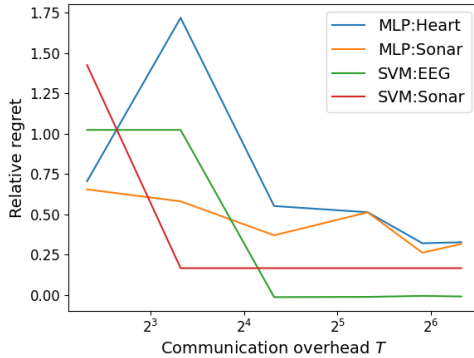
¹Moreover, [Khodak et al., 2021] claim that FedEx can handle architectural hyper-parameters but it is never demonstrated and discussed explicitly. In contrast, our proposed algorithm can handle architectural hyperparameters (as we do with HGB (tree depth) and MLP (width of the layer)).

Table 2: Effect of increasing the number of parties on FLoRA with different loss surfaces for HGB.

| Data | p | γ_p | SGM | SGM+U | MPLM | APLM |
|--------------------------------|-----|------------|------|-------|------|------|
| EEG Eye State 14980 samples | 3 | 1.01 | 0.14 | 0.12 | 0.11 | 0.12 |
| | 6 | 1.01 | 0.07 | 0.00 | 0.07 | 0.09 |
| | 10 | 1.03 | 0.08 | 0.00 | 0.16 | 0.01 |
| | 25 | 1.08 | 0.35 | 0.92 | 0.17 | 0.04 |
| | 50 | 1.20 | 0.20 | 0.23 | 0.67 | 0.12 |
| Electricity 45312 samples | 3 | 1.01 | 0.17 | 0.14 | 0.09 | 0.12 |
| | 6 | 1.01 | 0.25 | 0.21 | 0.18 | 0.13 |
| | 10 | 1.02 | 0.03 | 0.06 | 0.32 | 0.14 |
| | 25 | 1.04 | 0.40 | 0.42 | 1.42 | 0.89 |
| | 50 | 1.07 | 1.57 | 1.57 | 0.89 | 1.13 |
| | 100 | 1.14 | 1.45 | 1.47 | 0.48 | 1.11 |
| Pollen 3848 samples | 3 | 1.02 | 0.43 | 0.54 | 0.43 | 0.69 |
| | 6 | 1.10 | 1.02 | 0.91 | 0.54 | 0.56 |
| | 10 | 1.16 | 1.05 | 0.73 | 0.75 | 1.12 |



(a) # local HPO rounds.



(b) # (HP, loss) pairs communicated to aggregator

Figure 1: Effect of different choices on FLoRA with the APLM loss surface for different methods and datasets. More results and other loss surfaces are presented in Appendix C.4 and C.5.

ratio γ_p is always greater than 1, and highlights the difference in the observed performances across the parties. A ratio closer to 1 indicates that all the parties have relatively similar performances on their respective training data, while a ratio much higher than 1 indicating significant discrepancy between the per-party performances, implicitly indicating the difference in the per-party data distributions.

We notice that increasing the number of parties does not have a significant effect on γ_p for the Electricity dataset until $p = 100$, but significantly increases for the Pollen dataset earlier (making the problem harder). For the EEG eye state, the increase in γ_p with increasing p is moderate until $p = 50$. The results indicate that, with low or moderate increase in γ_p (EEG eye state, Electricity for moderate p), the proposed scheme is able to achieve low relative regret – the increase in the number of parties does not directly imply degradation in performance. However, with significant increase in γ_p (Pollen, Electricity with $p = 50, 100$ and EEG Eye State with $p = 50$), we see a significant increase in the relative regret (eventually going over 1 in a few cases). In this challenging case, MPLM (the most pessimistic loss function) has the most graceful degradation in relative regret compared to the remaining loss surfaces.

Effect of different choices in FLoRA. In this set of experiments, we consider FLoRA with the APLM loss surface, and ablate the effect of different choices in FLoRA on 2 datasets each for SVM and

Table 3: Performance of FLoRA with the IBM-FL system in terms of the *balanced accuracy* on a holdout test set (higher is better). The baseline is still the default HP configuration of HistGradientBoostingClassifier in scikit-learn.

| Data | # parties | # training data per party | Baseline | SGM | SGM+U | MPLM | APLM |
|---------------|-----------|---------------------------|----------|---------------|---------------|---------------|--------|
| Oil spill | 3 | 200 | 0.5895 | 0.7374 | 0.5909 | 0.7061 | 0.7332 |
| EEG eye state | 3 | 3,000 | 0.8864 | 0.9153 | 0.9211 | 0.9251 | 0.9245 |
| Electricity | 6 | 4,000 | 0.8448 | 0.8562 | 0.8627 | 0.8621 | 0.8624 |

MLP. First, we study the impact of the thoroughness of the per-party local HPOs, quantified by the number of HPO rounds T in Figure 1a. The results indicate that for really small T (< 20) the relative regret of FLoRA can be very high. However, after that point, the relative regret converges to its best possible value. We present the results for other loss surfaces in Appendix C.4.

We also study the effect of the communication overhead of FLoRA for fixed level of local HPO thoroughness. We assume that each party performs $T = 100$ rounds of local asynchronous HPO. However, instead of sending all T (HP, loss) pairs, we consider sending $T' < T$ of the “best” (HP, loss) pairs – that is, (HP, loss) pairs with the T' lowest losses. Changing the value of T' trades off the communication overhead of the FLoRA step where the aggregators collect the per-party loss pairs (Algorithm 1, line 5). The results for this study are presented in Figure 1b, and indicate that, for really small T' , the relative regret can be really high. However, for a moderately high value of $T' < T$, FLoRA converges to its best possible performance. Results on other loss surfaces and further discussion can be found in Appendix C.5.

Federated Learning testbed evaluation. We now conduct experiments for histogram boosted tree model in a FL testbed, utilizing IBM FL library [Ludwig et al., 2020, Ong et al., 2020], More specifically, we reserved 40% of oil spill and electricity and 20% of EEG eye state as global hold-out set only for evaluating the final FL model performance. Each party randomly sampled from the rest of the original dataset to obtain their own training dataset. We use the same HP search space as in Appendix C.2. We report the balanced accuracy of any HP (baseline or recommended by FLoRA) on a single train/test split. Given balanced accuracy as the evaluation metric, we utilize (1 - balanced accuracy) as the loss $\mathcal{L}_t^{(i)}$ in Algorithm 1 Each party will run HPO to generate $T = 500$ (HP, loss) pairs and use those pairs to generate loss surface either collaboratively or by their own according to different aggregation procedures described in §3.2. Once the loss surface is generated, the aggregator uses Hyperopt [Bergstra et al., 2011] to select the best HP candidate and train a federated XGBoost model via the IBM FL library using the selected HPs. Table 3 summarizes the experimental results for 3 datasets, indicating that FLoRA can significantly improve over the baseline in IBM FL testbed.

6 Conclusions

How to effectively select hyper-parameters in FL settings is a challenging problem. In this paper, we introduced FLoRA, a single-shot FL-HPO algorithm that can be applied to a variety of ML models. We provided a theoretical analysis which includes a bound on the optimality gap incurred by the hyper-parameter selection performed by FLoRA. Our experimental evaluation shows that FLoRA can effectively produce hyper-parameter configurations that outperform the baseline with just a single shot.

References

James Bergstra and Yoshua Bengio. Random search for hyper-parameter optimization. *Journal of Machine Learning Research*, 13(Feb):281–305, 2012.

- James S Bergstra, Rémi Bardenet, Yoshua Bengio, and Balázs Kégl. Algorithms for hyper-parameter optimization. In *Advances in neural information processing systems*, pages 2546–2554, 2011.
- Leo Breiman. Random forests. *Machine learning*, 45(1):5–32, 2001.
- Tianqi Chen and Carlos Guestrin. Xgboost: A scalable tree boosting system. In *Proceedings of the 22Nd ACM SIGKDD International Conference on Knowledge Discovery and Data Mining*, KDD '16, pages 785–794, New York, NY, USA, 2016. ACM. ISBN 978-1-4503-4232-2. doi: 10.1145/2939672.2939785. URL <http://doi.acm.org/10.1145/2939672.2939785>.
- Z. Dai, B.K.H. Low, and P. Jaillet. Federated bayesian optimization via thompson sampling. *Advances in Neural Information Processing Systems*, 33, 2020.
- Z. Dai, B.K.H. Low, and P. Jaillet. Differentially private federated bayesian optimization with distributed exploration. *Advances in Neural Information Processing Systems*, 34, 2021.
- Matthias Feurer, Aaron Klein, Katharina Eggensperger, Jost Springenberg, Manuel Blum, and Frank Hutter. Efficient and robust automated machine learning. In *Advances in Neural Information Processing Systems*, pages 2962–2970, 2015.
- Matthias Feurer, Katharina Eggensperger, Stefan Falkner, Marius Lindauer, and Frank Hutter. Auto-sklearn 2.0: The next generation. In *arXiv:2007.04074 [cs.LG]*, 2020.
- Jerome H Friedman. Greedy function approximation: a gradient boosting machine. *Annals of statistics*, pages 1189–1232, 2001.
- Anubhav Garg, Amit Kumar Saha, and Debo Dutta. Direct federated neural architecture search. *arxiv.2010.06223*, 2020.
- Chaoyang He, Murali Annavaram, and Salman Avestimehr. Towards non-i.i.d. and invisible data with fednas: Federated deep learning via neural architecture search. *arxiv.2004.08546*, 2020.
- Frank Hutter, Holger H Hoos, and Kevin Leyton-Brown. Sequential model-based optimization for general algorithm configuration. In *International Conference on Learning and Intelligent Optimization*, pages 507–523. Springer, 2011.
- Peter Kairouz, H Brendan McMahan, Brendan Avent, Aurélien Bellet, Mehdi Bennis, Arjun Nitin Bhagoji, Kallista Bonawitz, Zachary Charles, Graham Cormode, Rachel Cummings, et al. Advances and open problems in federated learning. *arXiv preprint arXiv:1912.04977*, 2019.
- Mikhail Khodak, Tian Li, Liam Li, M Balcan, Virginia Smith, and Ameet Talwalkar. Weight sharing for hyperparameter optimization in federated learning. In *Int. Workshop on Federated Learning for User Privacy and Data Confidentiality in Conjunction with ICML 2020*, 2020.
- Mikhail Khodak, Renbo Tu, Tian Li, Liam Li, Maria-Florina Balcan, Virginia Smith, and Ameet Talwalkar. Federated hyperparameter tuning: Challenges, baselines, and connections to weight-sharing. *arXiv preprint arXiv:2106.04502*, 2021.
- Diederik P. Kingma and Jimmy Ba. Adam: A method for stochastic optimization. In *ICLR (Poster)*, 2015. URL <http://arxiv.org/abs/1412.6980>.
- A. Koskela and A. Honkela. Learning rate adaptation for federated and differentially private learning. *arXiv preprint arXiv:1809.03832*, 2019.
- Heiko Ludwig, Nathalie Baracaldo, Gegi Thomas, Yi Zhou, Ali Anwar, Shashank Rajamoni, Yuya Ong, Jayaram Radhakrishnan, Ashish Verma, Mathieu Sinn, et al. IBM Federated Learning: an enterprise framework white paper v0. 1. *arXiv preprint arXiv:2007.10987*, 2020. URL <https://github.com/IBM/federated-learning-lib>.

- B. McMahan, E. Moore, D. Ramage, S. Hampson, and B. A. Arcas. Communication-efficient learning of deep networks from decentralized data. In *Proc. International Conference on Artificial Intelligence and Statistics*, pages 1273–1282, Ft. Lauderdale, FL, 20–22 Apr 2017a.
- Brendan McMahan, Eider Moore, Daniel Ramage, Seth Hampson, and Blaise Aguera y Arcas. Communication-efficient learning of deep networks from decentralized data. In *Artificial intelligence and statistics*, pages 1273–1282. PMLR, 2017b.
- H. Mostafa. Robust federated learning through representation matching and adaptive hyper-parameters. *arXiv preprint arXiv:1912.13075*, 2019.
- Changyong Oh, Jakub M Tomczak, Efstratios Gavves, and Max Welling. Combinatorial bayesian optimization using the graph cartesian product. In *Proceedings of the 33rd International Conference on Neural Information Processing Systems*, pages 2914–2924, 2019.
- Yuya Jeremy Ong, Yi Zhou, Nathalie Baracaldo, and Heiko Ludwig. Adaptive histogram-based gradient boosted trees for federated learning. *arXiv preprint arXiv:2012.06670*, 2020.
- F. Pedregosa, G. Varoquaux, A. Gramfort, V. Michel, B. Thirion, O. Grisel, M. Blondel, P. Prettenhofer, R. Weiss, V. Dubourg, J. Vanderplas, A. Passos, D. Cournapeau, M. Brucher, M. Perrot, and E. Duchesnay. Scikit-learn: Machine learning in Python. *Journal of Machine Learning Research*, 12: 2825–2830, 2011.
- S.J. Reddi, Z. Charles, M. Zaheer, Z. Garrett, K. Rush, J. Konecny, S. Kumar, and H.B. McMahan. Adaptive federated optimization. In *International Conference on Learning Representations*, 2020.
- B. Shahriari, K. Swersky, Z. Wang, R. P. Adams, and N. De Freitas. Taking the human out of the loop: A review of bayesian optimization. *Proceedings of the IEEE*, 104(1):148–175, 2016.
- Joaquin Vanschoren. Meta-learning: A survey. *arXiv preprint arXiv:1810.03548*, 2018.
- Joaquin Vanschoren, Jan N. van Rijn, Bernd Bischl, and Luis Torgo. OpenML: Networked science in machine learning. *SIGKDD Explorations*, 15(2):49–60, 2013. doi: 10.1145/2641190.2641198. URL <http://doi.acm.org/10.1145/2641190.2641198>.
- Cedric Villani. Topics in optimal transportation.(books). *OR/MS Today*, 30(3):66–67, 2003.
- Shiqiang Wang, Tiffany Tuor, Theodoros Salonidis, Kin Leung, Christian Makaya, Ting He, and Kevin Chan. Adaptive federated learning in resource constrained edge computing systems. *Journal Selected Areas in Communications (JSAC)*, 2019.
- Christopher K Williams and Carl Edward Rasmussen. *Gaussian processes for machine learning*, volume 2. MIT press Cambridge, MA, 2006.
- Martin Wistuba, Nicolas Schilling, and Lars Schmidt-Thieme. Scalable gaussian process-based transfer surrogates for hyperparameter optimization. *Machine Learning*, 107(1):43–78, 2018.
- Mengwei Xu, Yuxin Zhao, Kaigui Bian, Gang Huang, Qiaozhu Mei, and Xuanzhe Liu. Federated neural architecture search. *arxiv.2002.06352*, 2020.

A Technical Definitions

A.1 Distance in Θ

Here we will define a distance metric $d : \Theta \times \Theta \rightarrow \mathbb{R}_+$. Assuming we have m HPs, if $\Theta \subset \mathbb{R}^m$, then there are various distances available such as $\|\theta - \theta'\|_\rho$ (the ρ -norm). The more general case is where we have R continuous/real HPs, I integer HPs, and C categorical HPs; $m = R + I + C$. In that case, $\Theta \subset \mathbb{R}^R \times \mathbb{Z}^I \times \mathbb{C}^C$, and any $\theta = (\theta_{\mathbb{R}}, \theta_{\mathbb{Z}}, \theta_{\mathbb{C}}) \in \Theta_{\mathbb{R}} \times \Theta_{\mathbb{Z}} \times \Theta_{\mathbb{C}}$, where $\theta_{\mathbb{R}} \in \Theta_{\mathbb{R}}, \theta_{\mathbb{Z}} \in \Theta_{\mathbb{Z}}, \theta_{\mathbb{C}} \in \Theta_{\mathbb{C}}$ respectively denote the continuous, integer and categorical HPs in θ . Distances over $\mathbb{R}^R \times \mathbb{Z}^I$ is available, such as ρ -norm. Let $d_{\mathbb{R},\mathbb{Z}} : (\Theta_{\mathbb{R}} \times \Theta_{\mathbb{Z}}) \times (\Theta_{\mathbb{R}} \times \Theta_{\mathbb{Z}}) \rightarrow \mathbb{R}_+$ be some such distance.

To define distances over categorical spaces, there are some techniques such as one described by Oh et al. [2019]:

Assume that each of the C HPs $\theta_{\mathbb{C},k}, k \in [C]$ have n_k categories $\{\xi_{k1}, \xi_{k2}, \dots, \xi_{kn_k}\}$. Then we define a complete undirected graph $G_k = (V_k, E_k), k \in [C]$ where

- There is a node N_{kj} in G_k for each category ξ_{kj} for each $j \in [n_k]$ and $V_k = \{N_{k1}, \dots, N_{kn_k}\}$.
- There is an undirected edge $(N_{kj}, N_{kj'})$ for each pair $j, j' \in [n_k]$, and $E_k = \{(N_{kj}, N_{kj'}), j, j' \in [n_k]\}$.

Given the per-categorical HP graph $G_k, k \in [C]$, we define the graph Cartesian product $G = \bigotimes_{k \in [C]} G_k$ and $G = (V, E)$ such that

- $V = \{N_{(j_1, j_2, \dots, j_C)} : (\xi_{1j_1}, \xi_{2j_2}, \dots, \xi_{kj_k}, \dots, \xi_{Cj_C}) \in \Theta_{\mathbb{C}}, j_k \in [n_k] \forall k \in [C]\}$.
- $E = \{(N_{(j_1, j_2, \dots, j_C)}, N_{(j'_1, j'_2, \dots, j'_C)}) : \text{IFF} \exists t \in [C] \text{ such that } \forall k \neq t, \xi_{kj_k} = \xi_{kj'_k}, \text{ and } \exists (N_{tj_t}, N_{tj'_t}) \in E_t\}$.

Then for any $\theta_{\mathbb{C}}, \theta'_{\mathbb{C}} \in \Theta_{\mathbb{C}}$ with corresponding nodes $N, N' \in V$, Oh et al. [2019, Theorem 2.2.1] says that the length of the shortest path between nodes N and N' in G is a distance. We can consider this distance as $d_{\mathbb{C}} : \Theta_{\mathbb{C}} \times \Theta_{\mathbb{C}} \rightarrow \mathbb{R}_+$. Of course, there are other ways of defining distances in the categorical space.

Then we can define a distance $d : (\Theta_{\mathbb{R}} \times \Theta_{\mathbb{Z}} \times \Theta_{\mathbb{C}}) \times (\Theta_{\mathbb{R}} \times \Theta_{\mathbb{Z}} \times \Theta_{\mathbb{C}}) \rightarrow \mathbb{R}_+$ between two HPs θ, θ' as

$$d(\theta, \theta') = d_{\mathbb{R},\mathbb{Z}}((\theta_{\mathbb{R}}, \theta_{\mathbb{Z}}), (\theta'_{\mathbb{R}}, \theta'_{\mathbb{Z}})) + d_{\mathbb{C}}(\theta_{\mathbb{C}}, \theta'_{\mathbb{C}}). \quad (\text{A.1})$$

Proposition A.1. *Given distance metrics $d_{\mathbb{R},\mathbb{Z}}$ and $d_{\mathbb{C}}$, the function $d : \Theta \times \Theta$ defined in (A.1) is a valid distance metric.*

A.2 Continuity in the space of HPs Θ

In the simple case, we can assume Lipschitz continuity of estimated loss $\tilde{\ell}(\theta, \mathcal{D})$ and the loss surface $\hat{\ell}_i(\theta), i \in [p]$ as follows:

$$|\ell(\theta, \mathcal{D}) - \ell(\theta', \mathcal{D})| \leq \tilde{L}(\mathcal{D}) \cdot d(\theta, \theta'), \quad (\text{A.2})$$

$$|\hat{\ell}_i(\theta) - \hat{\ell}_i(\theta')| \leq \hat{L} \cdot d(\theta, \theta'). \quad (\text{A.3})$$

For a more general handling, we can consider the notion of modulus of continuity in the form of an increasing real-valued function $\omega : \mathbb{R}_+ \rightarrow \mathbb{R}_+$ with $\lim_{t \rightarrow 0} \omega(t) = \omega(0) = 0$. Then we can say that the estimated loss $\tilde{\ell}(\theta, \mathcal{D})$ and the loss surface $\ell_i(\theta)$ admits $\tilde{\omega}_{\mathcal{D}}$ and $\hat{\omega}$ as a modulus of continuity (respectively) if

$$|\ell(\theta, \mathcal{D}) - \ell(\theta', \mathcal{D})| \leq \tilde{\omega}_{\mathcal{D}}(d(\theta, \theta')) \quad (\text{A.4})$$

$$|\hat{\ell}_i(\theta) - \hat{\ell}_i(\theta')| \leq \hat{\omega}(d(\theta, \theta')). \quad (\text{A.5})$$

If we further assume that $\tilde{\omega}_{\mathcal{D}}, \hat{\omega}$ to be concave, then we can say that these functions are sublinear as follows:

$$\tilde{\omega}_{\mathcal{D}}(\mathbf{t}) \leq \tilde{\Lambda}_{\mathcal{D}} \cdot \mathbf{t} + \tilde{\mathbf{B}}_{\mathcal{D}}, \quad (\text{A.6})$$

$$\hat{\omega}(\mathbf{t}) \leq \hat{\Lambda} \cdot \mathbf{t} + \hat{\mathbf{B}}. \quad (\text{A.7})$$

These conditions give us (indirectly) something similar in spirit to the guarantees of Lipschitz continuity, but is a more rigorous way of achieving such guarantees.

B Proofs for optimality analysis

We provide detailed proofs of the propositions stated in Section 4.

B.1 Proof of Proposition 4.6

Proof. Consider the definition of $\hat{\boldsymbol{\theta}}^*$ and $\boldsymbol{\theta}^*$, we can obtain

$$\begin{aligned} \tilde{\ell}(\hat{\boldsymbol{\theta}}^*, \mathcal{D}) - \tilde{\ell}(\boldsymbol{\theta}^*, \mathcal{D}) &= \tilde{\ell}(\hat{\boldsymbol{\theta}}^*, \mathcal{D}) - \hat{\ell}(\hat{\boldsymbol{\theta}}^*) + \hat{\ell}(\hat{\boldsymbol{\theta}}^*) - \hat{\ell}(\boldsymbol{\theta}^*) + \hat{\ell}(\boldsymbol{\theta}^*) - \tilde{\ell}(\boldsymbol{\theta}^*, \mathcal{D}) \\ &\leq 2 \max_{\boldsymbol{\theta} \in \hat{\Theta} \subset \Theta} \left| \tilde{\ell}(\boldsymbol{\theta}, \mathcal{D}) - \hat{\ell}(\boldsymbol{\theta}) \right|, \end{aligned}$$

where the inequality follows from the fact that $\hat{\ell}(\hat{\boldsymbol{\theta}}^*) - \hat{\ell}(\boldsymbol{\theta}^*) \leq 0$. Moreover, observe that for any $\boldsymbol{\theta} \in \hat{\Theta} \subset \Theta$, by the definition of $\hat{\ell}(\boldsymbol{\theta})$ in (4.2), we have

$$\begin{aligned} |\tilde{\ell}(\boldsymbol{\theta}, \mathcal{D}) - \hat{\ell}(\boldsymbol{\theta})| &= \left| \tilde{\ell}(\boldsymbol{\theta}, \mathcal{D}) - \sum_{i \in [p]} \alpha_i(\boldsymbol{\theta}) \cdot \hat{\ell}_i(\boldsymbol{\theta}) \right| \\ &= \left| \tilde{\ell}(\boldsymbol{\theta}, \mathcal{D}) - \sum_{i \in [p]} \alpha_i(\boldsymbol{\theta}) \cdot \tilde{\ell}(\boldsymbol{\theta}, \mathcal{D}_i) + \sum_{i \in [p]} \alpha_i(\boldsymbol{\theta}) \cdot \tilde{\ell}(\boldsymbol{\theta}, \mathcal{D}_i) - \sum_{i \in [p]} \alpha_i(\boldsymbol{\theta}) \cdot \hat{\ell}_i(\boldsymbol{\theta}) \right| \\ &\leq \sum_{i \in [p]} \alpha_i(\boldsymbol{\theta}) \left| \tilde{\ell}(\boldsymbol{\theta}, \mathcal{D}) - \tilde{\ell}(\boldsymbol{\theta}, \mathcal{D}_i) \right| + \sum_{i \in [p]} \alpha_i(\boldsymbol{\theta}) \left| \tilde{\ell}(\boldsymbol{\theta}, \mathcal{D}_i) - \hat{\ell}_i(\boldsymbol{\theta}) \right| \\ &\leq \sum_{i \in [p]} \alpha_i(\boldsymbol{\theta}) \tilde{\beta}(\boldsymbol{\theta}) \mathcal{W}_1(\mathcal{D}, \mathcal{D}_i) + \sum_{i \in [p]} \alpha_i(\boldsymbol{\theta}) \epsilon_i(\boldsymbol{\theta}, \mathbb{T}), \end{aligned}$$

where the last inequality follows from assumption (4.6) and definition (4.10). \square

B.2 Proof of Proposition 4.7

Proof. By the definition of 1-Wasserstein distance in (4.3) and the fact that $\mathcal{D} = \sum_{i \in [p]} w_i \mathcal{D}_i$, we can obtain

$$\begin{aligned} \mathcal{W}_1(\mathcal{D}, \mathcal{D}_i) &= \sup_{f \in \mathcal{F}_1} \mathbb{E}_{(x, y) \sim \mathcal{D}} f(x, y) - \mathbb{E}_{(x_i, y_i) \sim \mathcal{D}_i} f(x_i, y_i) \\ &= \sup_{f \in \mathcal{F}_1} \sum_{j \in [p]} w_j \mathbb{E}_{(x_j, y_j) \sim \mathcal{D}_j} f(x_j, y_j) - \mathbb{E}_{(x_i, y_i) \sim \mathcal{D}_i} f(x_i, y_i) \\ &= \sup_{f \in \mathcal{F}_1} \sum_{i \neq j, j \in [p]} w_j \left(\mathbb{E}_{(x_j, y_j) \sim \mathcal{D}_j} f(x_j, y_j) - \mathbb{E}_{(x_i, y_i) \sim \mathcal{D}_i} f(x_i, y_i) \right) \\ &\leq \sum_{i \neq j, j \in [p]} w_j \left(\sup_{f \in \mathcal{F}_1} \mathbb{E}_{(x_j, y_j) \sim \mathcal{D}_j} f(x_j, y_j) - \mathbb{E}_{(x_i, y_i) \sim \mathcal{D}_i} f(x_i, y_i) \right) \\ &\leq \sum_{i \neq j, j \in [p]} w_j \mathcal{W}_1(\mathcal{D}_j, \mathcal{D}_i). \end{aligned}$$

\square

B.3 Proof of Proposition 4.8

Proof. By the definition of $\epsilon_i(\boldsymbol{\theta}, \mathbb{T})$

$$\begin{aligned} \epsilon_i(\boldsymbol{\theta}, \mathbb{T}) &= \left| \tilde{\ell}(\boldsymbol{\theta}, \mathcal{D}_i) - \widehat{\ell}_i(\boldsymbol{\theta}) \right| \\ &= \left| \underbrace{\tilde{\ell}(\boldsymbol{\theta}, \mathcal{D}_i) - \tilde{\ell}(\boldsymbol{\theta}_t^{(i)}, \mathcal{D}_i)}_{\text{Smoothness of } \tilde{\ell}} + \underbrace{\tilde{\ell}(\boldsymbol{\theta}_t^{(i)}, \mathcal{D}_i) - \widehat{\ell}_i(\boldsymbol{\theta}_t^{(i)})}_{\text{Modeling error}} + \underbrace{\widehat{\ell}_i(\boldsymbol{\theta}_t^{(i)}) - \widehat{\ell}_i(\boldsymbol{\theta})}_{\text{Smoothness of } \widehat{\ell}} \right|, \end{aligned}$$

where $\boldsymbol{\theta}_t^{(i)}, t \in [\mathbb{T}]$ is *any* one of the HP tried during local HPO run on party $i \in [p]$.

First note that

$$\begin{aligned} |\tilde{\ell}(\boldsymbol{\theta}_t^{(i)}, \mathcal{D}_i) - \widehat{\ell}_i(\boldsymbol{\theta}_t^{(i)})| &= |\mathcal{L}_t^{(i)} - \widehat{\ell}_i(\boldsymbol{\theta}_t^{(i)})| \\ &\leq \max_t |\mathcal{L}_t^{(i)} - \widehat{\ell}_i(\boldsymbol{\theta}_t^{(i)})| \\ &\leq \delta_i. \end{aligned}$$

In view of (4.4) and (4.6), we have

$$\epsilon_i(\boldsymbol{\theta}, \mathbb{T}) \leq \tilde{L}(\mathcal{D}_i) d(\boldsymbol{\theta}, \boldsymbol{\theta}_t^{(i)}) + \delta_i + \widehat{L}_i d(\boldsymbol{\theta}, \boldsymbol{\theta}_t^{(i)}),$$

which immediately implies the result in (4.13). \square

B.4 Proposition 4.8 using modulus of continuity instead of Lipschitz continuity

Proposition B.1. *Assume that the estimated loss $\tilde{\ell}(\boldsymbol{\theta}, \mathcal{D}_i)$ and the loss surface $\ell_i(\boldsymbol{\theta})$ admit concave functions $\tilde{\omega}_{\mathcal{D}_i}$ and $\widehat{\omega}_i$ respectively as a modulus of continuity with respect to $\boldsymbol{\theta} \in \Theta$ for each party $i \in [p]$. Then, for any party $i, i \in [p]$, with the set of (HP, loss) pairs $\{(\boldsymbol{\theta}_t^{(i)}, \mathcal{L}_t^{(i)})\}_{t \in [\mathbb{T}]}$ collected during the local HPO run for party i , for any $\boldsymbol{\theta} \in \bar{\Theta} \subset \Theta$, there exists $\tilde{A}_{\mathcal{D}_i}, \widehat{A}_i, \tilde{B}_{\mathcal{D}_i}, \widehat{B}_i \geq 0$ such that*

$$\epsilon_i(\boldsymbol{\theta}, \mathbb{T}) \leq \left(\tilde{A}_{\mathcal{D}_i} + \widehat{A}_i \right) \min_{t \in [\mathbb{T}]} d(\boldsymbol{\theta}, \boldsymbol{\theta}_t^{(i)}) + \tilde{B}_{\mathcal{D}_i} + \widehat{B}_i + \delta_i, \quad (\text{B.1})$$

where $\delta_i = \max_t |\mathcal{L}_t^{(i)} - \widehat{\ell}_i(\boldsymbol{\theta}_t^{(i)})|$ is the maximum per sample training error for the local loss surface $\widehat{\ell}_i$.

Proof. By the definition of $\epsilon_i(\boldsymbol{\theta}, \mathbb{T})$

$$\begin{aligned} \epsilon_i(\boldsymbol{\theta}, \mathbb{T}) &= \left| \tilde{\ell}(\boldsymbol{\theta}, \mathcal{D}_i) - \widehat{\ell}_i(\boldsymbol{\theta}) \right| \\ &= \left| \underbrace{\tilde{\ell}(\boldsymbol{\theta}, \mathcal{D}_i) - \tilde{\ell}(\boldsymbol{\theta}_t^{(i)}, \mathcal{D}_i)}_{\text{Smoothness of } \tilde{\ell}} + \underbrace{\tilde{\ell}(\boldsymbol{\theta}_t^{(i)}, \mathcal{D}_i) - \widehat{\ell}_i(\boldsymbol{\theta}_t^{(i)})}_{\text{Modeling error}} + \underbrace{\widehat{\ell}_i(\boldsymbol{\theta}_t^{(i)}) - \widehat{\ell}_i(\boldsymbol{\theta})}_{\text{Smoothness of } \widehat{\ell}} \right|, \end{aligned}$$

where $\boldsymbol{\theta}_t^{(i)}, t \in [\mathbb{T}]$ is *any* one of the HP tried during local HPO run on party $i \in [p]$.

First note that

$$\begin{aligned} |\tilde{\ell}(\boldsymbol{\theta}_t^{(i)}, \mathcal{D}_i) - \widehat{\ell}_i(\boldsymbol{\theta}_t^{(i)})| &= |\mathcal{L}_t^{(i)} - \widehat{\ell}_i(\boldsymbol{\theta}_t^{(i)})| \\ &\leq \max_t |\mathcal{L}_t^{(i)} - \widehat{\ell}_i(\boldsymbol{\theta}_t^{(i)})| \\ &\leq \delta_i. \end{aligned}$$

In view of (A.4) and (A.5), we have

$$\begin{aligned}\epsilon_i(\boldsymbol{\theta}, T) &\leq \tilde{\omega}_{\mathcal{D}_i}(\mathbf{d}(\boldsymbol{\theta}, \boldsymbol{\theta}_t^{(i)})) + \delta_i + \widehat{\omega}(\mathbf{d}(\boldsymbol{\theta}, \boldsymbol{\theta}_t^{(i)})), \\ &\leq \delta_i + \min_{t \in [T]} \left(\tilde{\omega}_{\mathcal{D}_i}(\mathbf{d}(\boldsymbol{\theta}, \boldsymbol{\theta}_t^{(i)})) + \widehat{\omega}(\mathbf{d}(\boldsymbol{\theta}, \boldsymbol{\theta}_t^{(i)})) \right).\end{aligned}$$

Concavity of a function $\omega : [0, \infty] \rightarrow [0, \infty]$ implies that there exists $A, B > 0$ such that $\omega(t) \leq At + B$. Using that, we can find some $\tilde{A}_{\mathcal{D}_i}, \widehat{A}_i, \tilde{B}_{\mathcal{D}_i}, \widehat{B}_i > 0$ which allows us to simplify the above to

$$\epsilon_i(\boldsymbol{\theta}, T) \leq \delta_i + (\tilde{A}_{\mathcal{D}_i} + \widehat{A}_i) \cdot \min_{t \in [T]} \mathbf{d}(\boldsymbol{\theta}, \boldsymbol{\theta}_t^{(i)}) + (\tilde{B}_{\mathcal{D}_i} + \widehat{B}_i).$$

□

B.5 Relative regrets

As a byproduct, we can also provide a bound for the following relative regret we use in our experiments.

Corollary B.2. *Let us assume $\widehat{\boldsymbol{\theta}}^*$ and $\boldsymbol{\theta}^*$ are defined in (3.7) and (4.7), and $\bar{\boldsymbol{\theta}}^*$ and $\boldsymbol{\theta}_b$ are the hyper-parameter settings selected by centralized HPO and some baseline hyper-parameters, respectively, then we can bound the relative regret as follows, for a given data distribution \mathcal{D} , we have*

$$\begin{aligned}&\frac{\tilde{\ell}(\bar{\boldsymbol{\theta}}^*, \mathcal{D}) - \tilde{\ell}(\widehat{\boldsymbol{\theta}}^*, \mathcal{D})}{\tilde{\ell}(\bar{\boldsymbol{\theta}}^*, \mathcal{D}) - \tilde{\ell}(\boldsymbol{\theta}_b, \mathcal{D})} \\ &\leq \frac{2 \max_{\boldsymbol{\theta} \in \bar{\Theta}} \sum_{i \in [p]} \alpha_i(\boldsymbol{\theta}) \left\{ \tilde{\beta}(\boldsymbol{\theta}) \sum_{j \in [p], j \neq i} w_j \mathcal{W}_1(\mathcal{D}_j, \mathcal{D}_i) + \left(\tilde{\mathbf{L}}(\mathcal{D}_i) + \widehat{\mathbf{L}}_i \right) \min_{t \in [T]} \mathbf{d}(\boldsymbol{\theta}, \boldsymbol{\theta}_t^{(i)}) + \delta_i \right\}}{\widehat{\ell}(\boldsymbol{\theta}_b, \mathcal{D}) - \widehat{\ell}(\bar{\boldsymbol{\theta}}^*, \mathcal{D})}.\end{aligned}\tag{B.2}$$

Proof. By the definition of relative regret, we have

$$\begin{aligned}\frac{\tilde{\ell}(\bar{\boldsymbol{\theta}}^*, \mathcal{D}) - \tilde{\ell}(\widehat{\boldsymbol{\theta}}^*, \mathcal{D})}{\tilde{\ell}(\bar{\boldsymbol{\theta}}^*, \mathcal{D}) - \tilde{\ell}(\boldsymbol{\theta}_b, \mathcal{D})} &= \frac{\tilde{\ell}(\widehat{\boldsymbol{\theta}}^*, \mathcal{D}) - \tilde{\ell}(\bar{\boldsymbol{\theta}}^*, \mathcal{D})}{\tilde{\ell}(\boldsymbol{\theta}_b, \mathcal{D}) - \tilde{\ell}(\bar{\boldsymbol{\theta}}^*, \mathcal{D})} \\ &\leq \frac{\tilde{\ell}(\widehat{\boldsymbol{\theta}}^*, \mathcal{D}) - \tilde{\ell}(\boldsymbol{\theta}^*, \mathcal{D})}{\widehat{\ell}(\boldsymbol{\theta}_b, \mathcal{D}) - \widehat{\ell}(\bar{\boldsymbol{\theta}}^*, \mathcal{D})},\end{aligned}$$

where the last inequality follows from the fact that $\boldsymbol{\theta}^*$ is the minimizer of $\tilde{\ell}(\boldsymbol{\theta}, \mathcal{D})$. Moreover, in view of the result in Theorem 4.5, the result in (B.2) follows. □

C Experimental Setting

C.1 Dataset details

The details of the binary classification datasets used in our evaluation is reported in Table 4. We report the 10-fold cross-validated balanced accuracy of the default HP configuration on each of datasets with centralized training. The ‘‘Gap’’ column for the results for all datasets and models in §C.3 denote the difference between the best 10-fold cross-validated balanced accuracy obtained via centralized HPO and the 10-fold cross-validated balanced accuracy of the default HP configuration.

C.2 Search space

We use the search space definition used in the NeurIPS 2020 Black-box optimization challenge (<https://bbochallenge.com/>), described in details in the API documentation².

²https://github.com/rdturnermtl/bbo_challenge_starter_kit/#configuration-space

Table 4: OpenML binary classification dataset details

| Data | rows | columns | class sizes |
|---------------|-------|---------|----------------|
| EEG eye state | 14980 | 14 | (8257, 6723) |
| Electricity | 45312 | 8 | (26075, 19237) |
| Heart statlog | 270 | 13 | (150, 120) |
| Oil spill | 937 | 49 | (896, 41) |
| Pollen | 3848 | 5 | (1924, 1924) |
| Sonar | 208 | 61 | (111, 97) |
| PC3 | 1563 | 37 | (1403, 160) |

C.2.1 Histogram based Gradient Boosted Trees

Given this format for defining the HPO search space, we utilize the following precise search space for the `HistGradientBoostingClassifier` in `scikit-learn`:

```
api_config = {
    "max_iter": {"type": "int", "space": "linear", "range": (10, 200)},
    "learning_rate": {"type": "real", "space": "log", "range": (1e-3, 1.0)},
    "min_samples_leaf": {"type": "int", "space": "linear", "range": (1, 40)},
    "l2_regularization": {"type": "real", "space": "log", "range": (1e-4, 1.0)},
}
```

The HP configuration we consider for the single-shot baseline described in §5 is as follows:

```
config = {
    "max_iter": 100,
    "learning_rate": 0.1,
    "min_samples_leaf": 20,
    "l2_regularization": 0,
}
```

C.2.2 Kernel SVM with RBF kernel

For `SVC(kernel="rbf")` in `scikit-learn`, we use the following search space:

```
api_config = {
    "C": {"type": "real", "space": "log", "range": (0.01, 1000.0)},
    "gamma": {"type": "real", "space": "log", "range": (1e-5, 10.0)},
    "tol": {"type": "real", "space": "log", "range": (1e-5, 1e-1)},
}
```

The single shot baseline we consider for `SVC` from `Auto-sklearn` [Feurer et al., 2015] is:

```
config = {
    "C": 1.0,
    "gamma": 0.1,
    "tol": 1e-3,
```

C.2.3 Multi-Layered Perceptrons

For the `MLPClassifier(solver="adam")` from `scikit-learn`, we consider both architectural HP such as `hidden-layer-sizes` as well as optimizer parameters such as `alpha` and `learning-rate-init` for the Adam optimizer [Kingma and Ba, 2015]. We consider the following search space:

```
api_config = {
    "hidden_layer_sizes": {"type": "int", "space": "linear", "range": (50, 200)},
    "alpha": {"type": "real", "space": "log", "range": (1e-5, 1e1)},
    "learning_rate_init": {"type": "real", "space": "log", "range": (1e-5, 1e-1)},
}
```

We utilize the following single shot baseline:

```
config = {
  "hidden_layer_sizes": 100,
  "alpha": 1e-4,
  "learning_rate_init": 1e-3,
}
```

We fix the remaining HPs of `MLPClassifier` as with values used by Auto-sklearn.

```
activation="relu",
early_stopping=True,
shuffle=True,
batch_size="auto",
tol=1e-4,
validation_fraction=0.1,
beta_1=0.9,
beta_2=0.999,
epsilon=1e-8,
```

C.3 Detailed results of comparison against baselines

Here we present the relevant details and the performance of FLoRA on the FL-HPO of (i) histograms based gradient boosted trees (HGB) in Table 5), (ii) nonlinear support vector machines (SVM) in Table 6, and (iii) multi-layered perceptrons (MLP) in Table 7. We use the search spaces and the single-shot baselines presented in §C.2. We utilize all 7 datasets for each of the method *except* for the Electricity dataset with SVM because of the infeasible amount of time taken by SVM on this dataset. For each setup, we report the following:

- Performance of the single-shot baseline (“SSBaseline”),
- the best centralized HPO performance (“Best”),
- the available “Gap” for improvement,
- the minimum accuracy of the best local HP across all parties “PMin” := $\min_{i \in [p]} \max_t (1 - \tilde{\ell}(\theta_t^{(i)}, \mathcal{D}_i))$
- the maximum accuracy of the best local HP across all parties “PMax” := $\max_{i \in [p]} \max_t (1 - \tilde{\ell}(\theta_t^{(i)}, \mathcal{D}_i))$
- $\gamma_p = \text{PMax}/\text{PMin}$, and finally
- the regret for each of the considered loss surfaces in FLoRA.

For each of the three methods, we also report the aggregate performance over all considered datasets in terms of mean \pm standard deviation (“mean \pm std”), inter-quartile range (“IQR”), Wins/Ties/Losses of FLoRA with respect to the single-shot baseline (“W/T/L”), and a one-sided Wilcoxon Signed Ranked Test of statistical significance (“WSRT”) with the null hypothesis that the median of the difference between the single-shot baseline and FLoRA is positive against the alternative that the difference is negative (implying FLoRA improves over the baseline).⁷ These aggregate metrics are collected in Table 8 along with a set of final aggregate metrics across all datasets and methods.

Table 5: HGB

| Data | SSBaseline | Best | Gap | PMin | PMax |
|---------------|------------|-------|-------|-------|-------|
| PC3 | 58.99 | 63.81 | 4.82 | 61.67 | 64.37 |
| Pollen | 48.86 | 52.21 | 3.35 | 51.83 | 52.64 |
| Electricity | 87.75 | 92.84 | 5.10 | 88.42 | 89.19 |
| Sonar | 87.43 | 91.25 | 3.82 | 83.75 | 88.33 |
| Heart Statlog | 79.42 | 85.58 | 6.17 | 78.00 | 86.50 |
| Oil Spill | 63.22 | 74.58 | 11.36 | 68.16 | 82.16 |
| EEG Eye State | 89.96 | 94.66 | 4.70 | 91.80 | 92.29 |

| Data | γ_p | SGM | SGM+U | MPLM | APLM |
|----------------|------------|--------------------|--------------------|--------------------|--------------------|
| PC3 | 1.04 | 0.66 | 0.72 | 0.39 | 0.38 |
| Pollen | 1.02 | 0.43 | 0.54 | 0.43 | 0.69 |
| Electricity | 1.01 | 0.17 | 0.14 | 0.09 | 0.12 |
| Sonar | 1.05 | 1.33 | 0.41 | 0.92 | 0.71 |
| Heart Statlog | 1.11 | 0.69 | 0.55 | 0.89 | 0.50 |
| Oil Spill | 1.21 | 0.47 | 1.13 | 0.46 | 0.61 |
| EEG Eye State | 1.01 | 0.14 | 0.12 | 0.11 | 0.12 |
| mean \pm std | | 0.56 \pm 0.37 | 0.52 \pm 0.32 | 0.47 \pm 0.31 | 0.45 \pm 0.23 |
| IQR | | [0.30, 0.47, 0.68] | [0.27, 0.54, 0.64] | [0.25, 0.43, 0.67] | [0.25, 0.50, 0.65] |
| WTL | | 6/0/1 | 6/0/1 | 7/0/0 | 7/0/0 |
| WSRT | | (26, 0.02126) | (27, 0.01400) | (28, 0.00898) | (28, 0.00898) |

HGB. The results in Table 5 indicate that, in almost all cases, with all loss functions, FLoRA is able to improve upon the baseline to varying degrees (there is only one case where SGM performs worse than the baseline on Sonar). On average (across the datasets), SGM+U, MPLM and APLM perform better than SGM as we expected. MPLM performs better than SGM both in terms of average and standard deviation. Looking at the individual datasets, we see that, for datasets with low γ_p (EEG eye state, Electricity), all the proposed loss surface have low relative regret, indicating that the problem is easier as expected. For datasets with high γ_p (Heart statlog, Oil spill), the relative regret of all loss surfaces are higher (but still much smaller than 1), indicating that our proposed single-shot scheme can show improvement even in cases where there is significant difference in the per-party losses (and hence datasets).

SVM. For SVM we continue with the datasets selected using HGB (datasets with a “Gap” of at least 3%). Of the 7 datasets (Table 4), we skip Electricity because it takes a prohibitively long time for SVM to be trained on this dataset with a single HP. So we consider 6 datasets in this evaluation and present the corresponding results in Table 6. Of the 6, note that 2 of these datasets (Pollen, Heart Statlog) have really small “Gap” (highlighted in red in Table 6). Moreover, 2 of the datasets (Heart statlog, Oil Spill) also have really high γ_p indicating a high level of heterogeneity between the per-party distributions (again highlighted in red). In this case, there are a couple of datasets (Oil Spill and Pollen) where FLoRA is unable to show any improvement over the single-shot baseline (see underlined entries in Table 6), but both these cases either have a small or moderate “Gap” and/or have a high γ_p . Moreover, in one case, MPLM incurs a regret of 6.8, but this is a case with really high $\gamma_p = 1.14$ – MPLM rejects any HP that has a low score in even one of the parties, and in that process reject all promising HPs since the local HPOs on these disparate distributions did not concentrate on the same region of the HP space, thereby incurring a high MPLM loss in almost all regions of the HP where some local HPO focused on. Other than these expected hard cases, FLoRA is able to improve upon the baseline in most cases, and achieve optimal performance (zero regret) in a few cases (EEG Eye State, Heart Statlog).

Table 6: SVM

| Data | SSBaseline | Best | Gap | PMin | PMax |
|---------------|------------|-------|-------|-------|-------|
| Pollen | 49.48 | 50.30 | 0.82 | 51.55 | 53.55 |
| Sonar | 80.20 | 89.29 | 9.09 | 83.33 | 87.92 |
| Heart Statlog | 83.67 | 84.92 | 1.25 | 77.00 | 88.00 |
| Oil Spill | 82.76 | 86.54 | 3.78 | 77.14 | 88.45 |
| EEG Eye State | 50.24 | 60.51 | 10.28 | 69.54 | 71.72 |
| PC3 | 74.03 | 77.96 | 3.92 | 75.26 | 76.95 |

| Data | γ_p | SGM | SGM+U | MPLM | APLM |
|----------------|------------|--------------------|--------------------|--------------------|--------------------|
| Pollen | 1.04 | <u>1.35</u> | <u>1.45</u> | <u>2.84</u> | <u>2.30</u> |
| Sonar | 1.06 | 0.17 | 0.17 | 0.27 | 0.17 |
| Heart Statlog | 1.14 | 0.00 | 0.00 | <u>6.80</u> | 0.67 |
| Oil Spill | 1.15 | <u>1.28</u> | <u>1.16</u> | <u>1.12</u> | 0.41 |
| EEG Eye State | 1.03 | -0.01 | -0.01 | -0.02 | -0.01 |
| PC3 | 1.02 | 0.59 | 0.79 | 0.70 | 0.79 |
| mean \pm std | | 0.56 \pm 0.57 | 0.59 \pm 0.58 | 1.95 \pm 2.35 | 0.72 \pm 0.76 |
| IQR | | [0.04, 0.38, 1.11] | [0.04, 0.48, 1.07] | [0.38, 0.91, 2.41] | [0.23, 0.54, 0.76] |
| WTL | | 4/0/2 | 4/0/2 | 3/0/3 | 5/0/1 |
| WSRT | | (18, 0.05793) | (17, 0.08648) | (9, 0.62342) | (15, 0.17272) |

MLP. We consider all 7 datasets for the evaluation of FLoRA on FL-HPO for MLP HPs and present the results in Table 7. As with SVM, there are a few datasets with a small room for improvement (“Gap”) and/or high γ_p , again highlighted in red in Table 7. In some of these cases, FLoRA is unable to improve upon the single-shot baseline (Pollen, EEG Eye State). Other than these hard cases, FLoRA again able to show significant improvement over the single-shot baseline, with APLM performing the best.

Aggregate. The results for all the methods and datasets are aggregated in Table 8. All FLoRA loss surfaces show strong performance with respect to the single-shot baseline, with significantly more wins than losses, and 3rd-quartile regret values less than 1 (indicating improvement over the baseline). All FLoRA loss surfaces have a p-value of less than 0.05, indicating that we can reject the null hypothesis. Overall, APLM shows the best performance over all loss surfaces, both in terms of Wins/Ties/Losses over the baseline as well as in terms of the Wilcoxon Signed Rank Test, with the highest statistic and a p-value close to 10^{-3} . APLM also has significantly lower 3rd-quartile than all other loss surfaces. MPLM appears to have the worst performance but much of that is attributable to the really high regret of 6.8 and 2.84 it received for SVM with Heart Statlog and Pollen (both hard cases as discussed earlier). Otherwise, MPLM performs second best both for FL-HPO with HGB and MLP.

C.4 Effect of the number of local HPO rounds per party

In this experiment, we report additional results to study the effect of the “thoroughness” of the local HPO runs (in terms of the number of HPO rounds T) on the overall performance of FLoRA for all the loss surfaces in Table 9. In almost all cases, FLoRA does not require T to be too large to get enough information about the local HPO loss surface to get to its best possible performance.

C.5 Effect of communication overhead

While in the previous experiment, we studied the effect of the thoroughness of the local HPO runs on the performance of FLoRA, here we consider a subtly different setup. We assume that each party performs $T = 100$ rounds of local asynchronous HPO. However, instead of sending all T (HP, loss) pairs,

Table 7: MLP-Adam

| Data | SSBaseline | Best | Gap | PMin | PMax |
|---------------|------------|-------|-------------|-------|-------|
| Pollen | 50.39 | 51.26 | 0.87 | 51.46 | 52.23 |
| Electricity | 76.95 | 78.06 | 1.11 | 77.01 | 77.39 |
| Sonar | 61.63 | 79.32 | 17.69 | 69.17 | 78.75 |
| Heart Statlog | 72.17 | 85.17 | 13.00 | 79.50 | 89.50 |
| Oil Spill | 50.00 | 65.22 | 15.22 | 54.83 | 63.63 |
| EEG Eye State | 49.99 | 51.66 | 1.67 | 50.02 | 51.84 |
| PC3 | 50.00 | 59.56 | 9.56 | 53.47 | 56.60 |

| Data | γ_p | SGM | SGM+U | MPLM | APLM |
|---------------|-------------|-------------|-------------|-------------|-------------|
| Pollen | 1.02 | <u>1.88</u> | <u>1.45</u> | <u>1.45</u> | <u>1.31</u> |
| Electricity | 1.00 | 0.24 | 0.41 | 0.16 | 0.53 |
| Sonar | 1.14 | 0.26 | 0.55 | 0.52 | 0.39 |
| Heart Statlog | 1.13 | 0.46 | 0.37 | 0.42 | 0.28 |
| Oil Spill | 1.16 | 0.80 | 1.03 | 1.00 | 0.79 |
| EEG Eye State | 1.04 | <u>0.99</u> | <u>0.99</u> | <u>0.99</u> | <u>0.99</u> |
| PC3 | 1.06 | 0.96 | 1.00 | 0.89 | 0.90 |

| | | | | | |
|----------|--|--------------------|--------------------|--------------------|--------------------|
| mean±std | | 0.80 ± 0.53 | 0.83 ± 0.37 | 0.78 ± 0.40 | 0.74 ± 0.34 |
| IQR | | [0.36, 0.80, 0.97] | [0.48, 0.99, 1.01] | [0.47, 0.89, 1.00] | [0.46, 0.79, 0.95] |
| WTL | | 6/0/1 | 4/1/2 | 5/1/1 | 6/0/1 |
| WSRT | | (21, 0.11836) | (15, 0.17272) | (18, 0.05793) | (24, 0.04548) |

we consider sending $T' < T$ of the “best” (HP, loss) pairs – that is, (HP, loss) pairs with the T' lowest losses. Changing the value of T' trades off the communication overhead of the FLoRA step where the aggregators collect the per-party loss pairs (Algorithm 1, line 5). We consider 2 datasets each for 2 of the methods (SVM, MLP) and all the loss surfaces for FLoRA, and report all the results in Table 10.

Table 8: Aggregate Table

| Agg. | Method | SGM | SGM+U | MPLM | APLM |
|--------------|---------|---------------------------|--------------------|--------------------|---------------------------|
| mean ± std. | HGB | 0.56 ± 0.37 | 0.52 ± 0.32 | 0.47 ± 0.31 | 0.45 ± 0.23 |
| | SVM | 0.56 ± 0.57 | 0.59 ± 0.58 | 1.95 ± 2.35 | 0.72 ± 0.76 |
| | MLP | 0.80 ± 0.53 | 0.83 ± 0.37 | 0.78 ± 0.40 | 0.74 ± 0.34 |
| | Overall | 0.64 ± 0.51 | 0.64 ± 0.51 | 1.02 ± 1.46 | 0.63 ± 0.50 |
| IQR | HGB | [0.30, 0.47, 0.68] | [0.27, 0.54, 0.64] | [0.25, 0.43, 0.67] | [0.25, 0.50, 0.65] |
| | SVM | [0.04, 0.38, 1.11] | [0.04, 0.48, 1.07] | [0.38, 0.91, 2.41] | [0.23, 0.54, 0.76] |
| | MLP | [0.36, 0.80, 0.97] | [0.48, 0.99, 1.01] | [0.47, 0.89, 1.00] | [0.46, 0.79, 0.95] |
| | Overall | [0.22, 0.53, 0.97] | [0.32, 0.55, 1.01] | [0.36, 0.61, 0.99] | [0.36, 0.57, 0.79] |
| W/T/L | HGB | 6/0/1 | 6/0/1 | 7/0/0 | 7/0/0 |
| | SVM | 4/0/2 | 4/0/2 | 3/0/3 | 5/0/1 |
| | MLP | 6/0/1 | 4/1/2 | 5/1/1 | 6/0/1 |
| | Overall | 16/0/4 | 14/1/5 | 15/1/4 | 18/0/2 |
| WSRT 1 sided | HGB | (26, 0.02126) | (27, 0.01400) | (28, 0.00898) | (28, 0.00898) |
| | SVM | (18, 0.05793) | (17, 0.08648) | (9, 0.62342) | (15, 0.17272) |
| | MLP | (21, 0.11836) | (15, 0.17272) | (18, 0.05793) | (24, 0.04548) |
| | Overall | (174, 0.00499) | (164, 0.00272) | (141, 0.03206) | (183.5, 0.00169) |

Table 9: Effect of T.

| Method | data | T | γ_p | SGM | SGM+U | MPLM | APLM |
|--------|---------------|----|------------|-------|-------|-------|-------|
| MLP | Heart Statlog | 5 | 1.13 | 0.58 | 0.33 | 0.22 | 0.56 |
| | | 10 | 1.13 | 0.33 | 0.16 | 0.60 | 0.39 |
| | | 20 | 1.13 | 0.49 | 0.15 | 0.24 | 0.44 |
| | | 40 | 1.13 | 0.44 | 0.30 | 0.42 | 0.29 |
| | | 60 | 1.13 | 0.37 | 0.15 | 0.33 | 0.22 |
| | | 80 | 1.13 | 0.35 | 0.40 | 0.35 | 0.26 |
| MLP | Sonar | 5 | 1.14 | 0.38 | 0.38 | 0.51 | 0.78 |
| | | 10 | 1.14 | 0.45 | 0.23 | 0.43 | 0.62 |
| | | 20 | 1.14 | 0.39 | 0.24 | 0.36 | 0.30 |
| | | 40 | 1.14 | 0.23 | 0.37 | 0.65 | 0.49 |
| | | 60 | 1.14 | 0.53 | 0.14 | 0.34 | 0.48 |
| | | 80 | 1.14 | 0.46 | 0.07 | 0.19 | 0.30 |
| SVM | Sonar | 5 | 1.06 | 0.17 | 0.17 | 1.16 | 0.28 |
| | | 10 | 1.06 | 0.17 | 0.43 | 0.34 | 0.27 |
| | | 20 | 1.06 | 0.17 | 0.17 | 0.17 | 0.17 |
| | | 40 | 1.06 | 0.17 | 0.17 | 0.22 | 0.27 |
| | | 60 | 1.06 | 0.17 | 0.17 | 0.17 | 0.17 |
| | | 80 | 1.06 | 0.17 | 0.11 | 0.27 | 0.17 |
| SVM | EEG | 5 | 1.03 | -0.01 | -0.01 | 0.92 | 0.16 |
| | | 10 | 1.03 | -0.01 | -0.01 | -0.01 | 0.14 |
| | | 20 | 1.03 | -0.01 | -0.01 | -0.00 | -0.00 |
| | | 40 | 1.03 | -0.02 | -0.02 | 0.01 | 0.00 |
| | | 60 | 1.03 | -0.01 | -0.01 | 0.02 | 0.03 |
| | | 80 | 1.03 | -0.01 | -0.01 | 0.01 | -0.04 |

Table 10: Effect of the number of best (HP, loss) pairs $T' < T$ sent to aggregator by each party after doing local HPO with $T = 100$.

| Method | data | $T' < T$ | γ_p | SGM | SGM+U | MPLM | APLM |
|--------|---------------|----------|------------|-------|-------|-------|-------|
| MLP | Heart Statlog | 5 | 1.13 | 0.33 | 0.27 | 0.38 | 0.71 |
| | | 10 | 1.13 | 0.35 | 0.31 | 0.33 | 1.72 |
| | | 20 | 1.13 | 0.42 | 0.39 | 2.02 | 0.55 |
| | | 40 | 1.13 | 0.34 | 0.44 | 0.88 | 0.51 |
| | | 60 | 1.13 | 0.38 | 0.22 | 0.31 | 0.32 |
| | | 80 | 1.13 | 0.34 | 0.38 | 0.22 | 0.33 |
| MLP | Sonar | 5 | 1.14 | 0.39 | 0.50 | 1.78 | 0.65 |
| | | 10 | 1.14 | 0.73 | 0.18 | 1.66 | 0.58 |
| | | 20 | 1.14 | 0.20 | 0.41 | 1.23 | 0.37 |
| | | 40 | 1.14 | 0.60 | 0.42 | 0.18 | 0.51 |
| | | 60 | 1.14 | 0.10 | 0.33 | 0.55 | 0.26 |
| | | 80 | 1.14 | 0.47 | 0.41 | 0.34 | 0.32 |
| SVM | EEG Eye State | 5 | 1.03 | -0.02 | -0.01 | 0.39 | 1.02 |
| | | 10 | 1.03 | -0.01 | -0.01 | 1.02 | 1.02 |
| | | 20 | 1.03 | -0.01 | -0.01 | 0.01 | -0.01 |
| | | 40 | 1.03 | -0.01 | -0.01 | -0.00 | -0.01 |
| | | 60 | 1.03 | -0.01 | -0.01 | -0.01 | -0.01 |
| | | 80 | 1.03 | -0.01 | -0.01 | -0.01 | -0.01 |
| SVM | Sonar | 5 | 1.06 | 0.17 | 0.17 | 0.43 | 1.43 |
| | | 10 | 1.06 | 0.17 | 0.17 | 0.17 | 0.17 |
| | | 20 | 1.06 | 0.17 | 0.17 | 0.22 | 0.17 |
| | | 40 | 1.06 | 0.17 | 0.38 | 0.27 | 0.17 |
| | | 60 | 1.06 | 0.17 | 0.43 | 0.27 | 0.17 |
| | | 80 | 1.06 | 0.17 | 0.43 | 0.27 | 0.17 |